PREDICTION AND DETERMINANTS OF FOREARM FORCES DURING A FALL ON THE OUTSTRETCHED HAND: A PILOT STUDY

A Thesis Proposal Submitted to the

College of Kinesiology

in Partial Fulfillment of the Requirements

for the Degree of Master of Science

in the College of Kinesiology

University of Saskatchewan

Saskatoon

By

Chantal E. Kawalilak

PERMISSION TO USE

In presenting this thesis/dissertation in partial fulfillment of the requirements for a postgraduate degree from the University of Saskatchewan, I agree that the libraries of this university may make it freely available for inspection. I further agree that permission for copying of this thesis/dissertation in any manner, in whole or in part, for scholarly purposes may be granted by the professor or professors who supervised my thesis/dissertation work or, in their absence, by the head of the department or the dean of the college in which my thesis work was done. It is understood that any copying or publication or use of this thesis/dissertation or parts thereof for financial gain shall not be allowed without my written permission. It is also understood that due recognition shall be given to me and to the University of Saskatchewan in any scholarly use which may be made of any material in my thesis/dissertation.

Requests for permission to copy or to make other uses of materials in this thesis/dissertation in whole or part should be addressed to:

Dean of the College of Kinesiology

University of Saskatchewan

Saskatoon, Saskatchewan

S7N 5B2

ABSTRACT

Introduction. Wrist (Colles') and forearm fractures commonly occur when a person falls on the outstretched forearm and the force exceeds bone strength. There is lack of experimental evidence testing the available force prediction models and assessing factors that determine forearm forces during a fall.

Objective. The primary objective was to compare experimentally measured force peaks ($F_{1max\text{-}E}$ and $F_{2max\text{-}E}$) to the force peaks that were predicted by an engineering based force prediction model ($F_{1max\text{-}M}$ and $F_{2max\text{-}M}$), at heights greater than 5cm. The second objective was to describe the relationships between the experimentally measured peak forces and forearm bone and muscle strength properties, body mass, and stature as a function of fall height.

Methods. Using 3D motion tracking, we assessed the first (F_{1max}) and second (F_{2max}) peak forces from 10 young adults (5 male; 5 female) who volunteered to fall from heights up to 25cm onto a foam covered force plate. Peripheral QCT was used to determine the bone strength index (BSI_c), strength-strain index (SSI_p), and muscle cross sectional area (MCSA) of each participant. Two 2x8 between-within factorial ANOVAs determined the difference between the experimental and model force peaks, with post hoc analyses at all fall heights. Pearson's correlation was used to determine the relationship between the pQCT-derived bone and muscle strength indices and the force peaks.

Results. There was no significant differences between $F_{1max\text{-}E}$ and $F_{1max\text{-}M}$ across all fall heights, but the model significantly over-predicted the $F_{2max\text{-}E}$ across all fall heights. After controlling $F_{1max\text{-}E}$ and $F_{2max\text{-}E}$ for body mass, the force peaks appeared to be weakly related to the anthropometric as well as bone and muscle strength outcomes ($r=0.2\text{-}0.7$, $p>0.05$). The relationship between bone and muscle strength outcomes appeared to have a tendency to get stronger at higher fall heights.

Conclusion. The model predicted experimental F_{1max}, but not experimental F_{2max}. This study presents preliminary pilot results. Larger sample size is needed to confirm whether incorporating bone and muscle strength estimates into fall force prediction models could enhance forearm fracture risk assessments.

ACKNOWLEDGEMENTS

I would like to extend gratitude and sincere thanks to all those individuals who have made the completion of this thesis possible. Foremost I would like to thank Dr. Saija Kontulainen for being an insightful supervisor. Her guidance, support, and knowledge were invaluable throughout this process. I greatly appreciate her patience regarding my *many* inquiries and numerous thesis revisions.

I would also like to thank my committee members: Dr. Joel Lanovaz and Dr. Adam Baxter-Jones for their time, expertise, and valuable contributions. I would particularly like to extend magnanimous amounts of thanks and appreciation to Dr. Joel Lanovaz for the patience and guidance he bestowed on me, especially regarding the programming of Matlab and in the understanding of the mathematical model used in my thesis. Further, I would like to thank my external examiner, Dr. Vanina Dal Bello-Haas for her feedback.

I would like to recognize the engineering students: Devin Glennie, Jon Aydt, and Yi Liu, who developed and constructed the fall-release apparatus as part of their mechanical engineering design course, under the supervision of J.D. Johnston. I would especially like to thank Devin Glennie, J.D. Johnston, and Dr. Joel Lanovaz for writing the Matlab code used for the mathematical model. Additionally, I would like to thank David Kobylak who operated the Vicon system during my data collection. I am indebted to you all, for your hard work.

To my wonderful husband, Sheldon, I would like to extend exuberant amounts of gratitude for all of his patience, encouragement, and unending support. Thank you for enduring all of my ups and downs associated with writing this thesis. Additionally, I would like to greatly thank my participants, who are also my highly valued colleagues. Their unquestionable assistance in my time of need was greatly appreciated and will never be forgotten!

Finally, I would like to thank the University of Saskatchewan and the Canadian Institute of Health Research (CIHR) for funding me throughout my Master's program.

TABLE OF CONTENTS

LIST OF TABLES

LIST OF FIGURES

LIST OF EQUATIONS

LIST OF ABBREVIATIONS

Mathematical Model

$\mathbf{b_s}$	Damping variable for the shoulder (kN•s/m)
$\mathbf{b_w}$	Damping variable for the wrist (kN•s/m)
$\mathbf{F_{1max}}$	Initial high frequency peak force (N) for the experiment (E) or model (M)
$\mathbf{F_{2max}}$	Subsequent low frequency oscillatory peak force (N) for the experiment (E) or model (M)
GRF	Ground Reaction Force, used interchangeably with force (N)
$\mathbf{k_s}$	Stiffness of the shoulder (kN/m)
$\mathbf{k_w}$	Stiffness of the wrist (kN/m)
$\mathbf{k_g}$	Stiffness of the mat (kN/m)
$\mathbf{m_{torso}}$	Mass of the torso (49% total body mass, kg)
$\mathbf{m_{arm}}$	Mass of the arm (5% total body mass, kg)
$\mathbf{x_s}$	Displacement of the shoulder (m)
$\mathbf{x_w}$	Displacement of the wrist (m)
$\mathbf{x_g}$	Displacement of the mat (m)
$\mathbf{(x_s - x_w)}$	Shoulder deflection (m)
$\mathbf{(x_w - x_g)}$	Wrist deflection (m)
$\dot{x}$	Velocity of the given subscript (shoulder, *s*; wrist, *w*; mat, *g*) (m/s)
$\ddot{x}$	Acceleration of the given subscript (m/s^2)

Bone Related Properties

a	Area of the voxel (mm^2)
aBMD	Areal Bone Mineral Density (mg/cm^2)
BMC	Bone Mineral Content (g)
BSI_c	Bone Strength Index in Compression (mg^2/cm^4)
CoA	Cortical Area (mm^2)
CoD	Cortical Density (mg/cm^3)
d	Distance of the voxel of interest from the neutral axis (mm)
d_{max}	Distance of the farthest voxel from the neutral axis (mm)
DXA	Dual-energy X-ray Absorptiometry
MCSA	Muscle Cross Sectional Area (mm^2)
ND	Normal physiological Density (1200 mg/cm^2)
NCRP	National Council on Radiation Protection and Measurements
pQCT	Peripheral Quantitative Computed Tomography
SSI_p	Polar Strength Strain Index (mm^3)
ToA	Total Area (mm^2)
ToD	Total Density (mg/cm^3)
vBMD	Volumetric Bone Mineral Density (mg/cm^3)

LIST OF APPENDICES

LIST OF APPENDED TABLES

LIST OF APPENDED FIGURES

LIST OF DEFINITIONS

In this study, I will use a number of terms that may not be apparent to some readers. I have provided a list of definitions to clarify the use of terminology in this dissertation.

General Definitions:

Bone strength – The ability of the bone to withstand deformation as a load or force is applied to it (Seeman & Delmas, 2006).

Determinant – Refers to any factor that can be related or affect some other factor or condition (Vincent, 2005).

Estimate – Refers to the approximation of bone and muscle parameters using medical imaging (Seeman, 2001). In this study, I will use "estimate" as a surrogate for "prediction" when referring to bone and muscle parameters.

Force – Refers to the measure of the interaction between two objects (Serway & Jewett Jr., 2004)

Load – Refers to the force applied to an object (i.e., bone) (Serway & Jewett Jr., 2004)

Prediction – Refers to the process of determining the magnitude of variable (i.e., force) without experimentally collecting data pertaining to the variable (i.e., force) (Vincent, 2005).

Specific Definitions:

Failure load – Refers to the load required to break a bone *ex vivo* or estimated using finite element analysis (simulation) (Augat, 1998, MacNeil & Boyd, 2008).

Force – Refers to the force of the body being applied to the ground at impact. The magnitude of the body's force is equal to, but in the opposite direction from, the ground reaction force (GRF) (Serway & Jewett Jr., 2004). The GRF is the "force" that can be measured using a force plate and is the force that is applied to the hand of the outstretched forearm. In this dissertation I will use *force* to refer to the GRF.

Fracture load – Refers to the load required to initialize the breaking of a bone *in vivo* (Melton III et al, 2007).

Applied load – Refers to the load that the bone is subjected to prior to breaking, either *in vivo* or ex *vivo* (Augat, 1998, MacNeil & Boyd, 2008). This includes, but is not limited to: fall related forces and physical activity (Davidson et al., 2006).

1.0 INTRODUCTION

Fractures of the forearm are common in children and postmenopausal women (Burge et al., 2007; Chung & Spilson, 2001; Johnell & Kanis, 2006; Kawalilak, Baxter-Jones, Faulkner, Bailey, & Kontulainen, 2010; Landin, 2010; Rennie, Court-Brown, Mok, & Beattie, 2007). Previous research indicates that wrist and forearm fractures are an early indicator of bone fragility (Barrett-Connor et al., 2008; Ferrari, Chevalley, Bonjour, & Rizzoli, 2006; Klotzbuecher, Ross, Landsman, Abbott, & Berger, 2000; Schousboe et al., 2005). In children, previous wrist fracture is associated with lower pubertal bone mass accrual in the axial and appendicular skeleton (Ferrari et al., 2006). Further, peri-menopausal women who sustain a wrist or forearm fracture have an approximate 72% increased probability of sustaining a vertebral fracture within the next 10 years (Schousboe et al., 2005).

Forearm or wrist fractures occur when the force applied to the bone creates a stress within the bone tissue that exceeds the bone strength – usually due to standing height falls on the outstretched hand and forearm (Augat, Iida, Jiang, Diao, & Genant, 1998; Chiu & Robinovitch, 1998; Chung & Spilson, 2001; Cummings & Nevitt, 1994; Martin, Burr, & Sharkey, 1998; Melone, 1984). Previous *ex vivo* research has proposed that fracture risk is determined using the ratio of the applied load to the strength of the bone (Hayes, Piazza, & Zysset, 1991). Fracture is more than likely to occur if the ratio of applied load to bone strength is greater than 1.0, the theoretical mechanical fracture threshold (Keaveny & Bouxsein, 2008). Thus, strategies for preventing wrist and forearm fractures should focus on: fall prevention to avoid sustaining the ensuing fall related forces, reducing the fall related forces when a fall does occur, and enhancing bone and muscle strength in order to better withstand the forces when a fall occurs. Understanding the factors that predict and determine the fall related forces and bone strength are essential for optimizing wrist and forearm fracture prevention strategies. My thesis will focus on the forces that are applied to the hand of the outstretched forearm. I am particularly interested in the prediction of the forces, as well as the determining factors of the forces on the outstretched hand and forearm when a person falls from standing height.

The forces experienced during a fall onto the hand of the outstretched forearm have previously been attempted to be predicted using a mathematical model using engineering principles. Falling onto the outstretched forearm represents the worst case falling scenario (Chiu & Robinovitch, 1998). Prediction models are needed, as direct or experimental measures of the forces from standing heights can be unsafe, especially in older individuals. These mathematical models can provide safe estimations for fall related forces and may be used to augment fracture risk prediction. "Safe" is a term used to highlight the discretion of preventing fall related fractures, and other skeletal or soft tissue injuries that may be associated with direct measures of forces. A two-mass, spring-damper model is considered to be the simplest mathematical model representing the torso and arm during a fall (Chiu & Robinovitch, 1998). This model is based on engineering principles, using two masses connected by springs and dampers, to recreate the response of the torso and upper extremity during a fall. The model is used to predict the forces that are transmitted through the upper extremity during a fall on the outstretched forearm of adults (Chiu & Robinovitch, 1998; Robinovitch & Chiu, 1998).

The two-mass, spring-damper model has been used to predict forces at the hand of the outstretched forearm from standing heights in young adult males and females (mean age (±SD): 26±4.6 years) (Chiu & Robinovitch, 1998). The prediction results indicate that the peak force will exceed the average fracture force for the elderly radius at fall heights greater than 50 cm (Chiu & Robinovitch, 1998). The most commonly reported fracture force for the elderly radius is 2.26±1.0 kN (Frykman, 1967); more recent evidence suggests a range between 1.64 – 3.39 kN, for elderly radius fracture force (P. Augat, Iida et al., 1998; Muller, Webber, & Bouxsein, 2003; Myers et al., 1991; Myers, Hecker, Rooks, Hipp, & Hayes, 1993; Spadaro et al., 1994). The experimental evidence supporting the model prediction accuracy of standing height falls is limited to low fall heights of 1, 3, and 5 cm (Chiu & Robinovitch, 1998). The relationship of force at impact to fall height for falls from heights greater than 5 cm, may not be well represented from 3, low fall heights; consequently, the model predictions may not compare to the experimental forces at higher fall heights. Therefore, safe (i.e., lower than the fall heights associated with forearm fracture in the elderly radius) and higher fall heights are needed to further test the ability of the two-mass, spring-

damper model to predict the forces on the hand of the outstretched forearm at higher falling heights.

In addition to valid predictions of the fall induced forces, there is a need to characterize the factors that determine the magnitude of these forces when a person falls on the outstretched forearm and hand. Chiu and Robinovitch (1998) were the first to report force data on the upper limb using the two-mass, spring-damper model. Body mass was reported to be a dominant predictor of the forces involved in forward directed falls onto the hand of the outstretched forearm (Chiu & Robinovitch, 1998). Other studies used the two-mass, spring-damper model to determine: how surface stiffness influences the forces (Robinovitch & Chiu, 1998), how different angles at the elbow would alter the forces (DeGoede & Ashton-Miller, 2002), and the difference in impact velocities acting on the wrist between forwards and backwards falls (Tan, Eng, Robinovitch, & Warnick, 2006). However, there is no evidence available to indicate whether estimates of bone and muscle strength are related to forces, especially as the fall height increases. It would be prudent to consider the relationship between bone and muscle strength estimates and forces associated with forward directed falls because mechanical loads are transmitted to and absorbed within the bone and muscle (Nikander, Sievanen, Uusi-Rasi, Heinonen, & Kannus, 2006). Further, based on the premise: *Stress = Force/Area*, an increase in the bone and muscle area would decrease ihe stress within the bone and muscle and consequently decrease the risk of fracture (Kontulainen et al., 2008).

Therefore, my primary objective is to compare experimentally measured force peaks ($F_{1max\text{-}E}$ and $F_{2max\text{-}E}$) to the force peaks that will be predicted by the simulation model ($F_{1max\text{-}M}$ and $F_{2max\text{-}M}$), at higher fall heights than previously reported (i.e., >5 cm). I hypothesize that the experimentally measured peak forces ($F_{1max\text{-}E}$ and $F_{2max\text{-}E}$) will be comparable to the model simulated forces ($F_{2max\text{-}M}$ and $F_{2max\text{-}M}$) at higher fall heights than 5 cm, when using the generic spring and damping parameters in the model. My second objective is to describe the relationships between the experimentally measured peak forces ($F_{1max\text{-}E}$ and $F_{2max\text{-}E}$) and forearm bone and muscle properties, body mass, and stature as a function of fall height. I am particularly interested in describing whether estimates of muscle and bone strength may provide more predictive capacity of fall related forces on the hand of the outstretched

forearm over and above that of body mass. I hypothesize that $F_{1max\text{-}E}$ and $F_{2max\text{-}E}$ will be correlated to bone and muscle strength estimates, body mass and stature, and these correlations will increase with increasing fall heights.

2.0 REVIEW OF LITERATURE

Fractures of the forearm are common in children and postmenopausal women (Burge et al., 2007; Chung & Spilson, 2001; Johnell & Kanis, 2006; Kawalilak et al., 2010; Landin, 2010; Rennie et al., 2007). Further, the incidence of pediatric and osteoporotic forearm fractures has increased over the past 3 decades (Khosla et al., 2003; B. L. Riggs & Melton, 1995). Previous research has indicated that wrist and forearm fractures are an early indicator of bone fragility (Barrett-Connor et al., 2008; Ferrari et al., 2006; Klotzbuecher et al., 2000; Schousboe et al., 2005). In children, previous wrist fracture is associated with lower pubertal bone mass accrual in the axial and appendicular skeleton (Ferrari et al., 2006). Further, peri-menopausal women who sustain a wrist or forearm fracture have an approximate 72% increased probability of sustaining a vertebral fracture within the next 10 years (Schousboe et al., 2005). The number of osteoporotic fractures have been projected to continue increasing for the next 20 years (Burge et al., 2007). As of 2005, the medical cost of osteoporotic fractures was estimated to range between 13.7-20.3 billion dollars in the United States alone (Burge et al., 2007).

Understanding the fracture mechanism is essential for optimizing wrist and forearm fracture prevention. The risk of sustaining a fracture increases when the ratio of applied load to bone strength approaches 1.0, and fracture results when the applied load is larger than the strength of the bone (i.e., applied load : bone strength > 1.0) (W. C. Hayes et al., 1991; Keaveny & Bouxsein, 2008; Macdonald, Nishiyama, Kang, Hanley, & Boyd, 2010; Melton III et al., 2007) (Figure 1). The primary focus of my thesis will be on the forces that are applied to the hand of the outstretched forearm during a forward directed fall. I am particularly interested in the prediction of these forces. Further, I am interested in describing the relationship between the forces applied to the hand of the outstretched forearm and estimates of bone and muscle strength. I have provided an overview illustrating the direction of the ensuing literature review (Figure 1). In the following sections, I will introduce and discuss the key factors determining fracture risk: the applied load and bone strength.

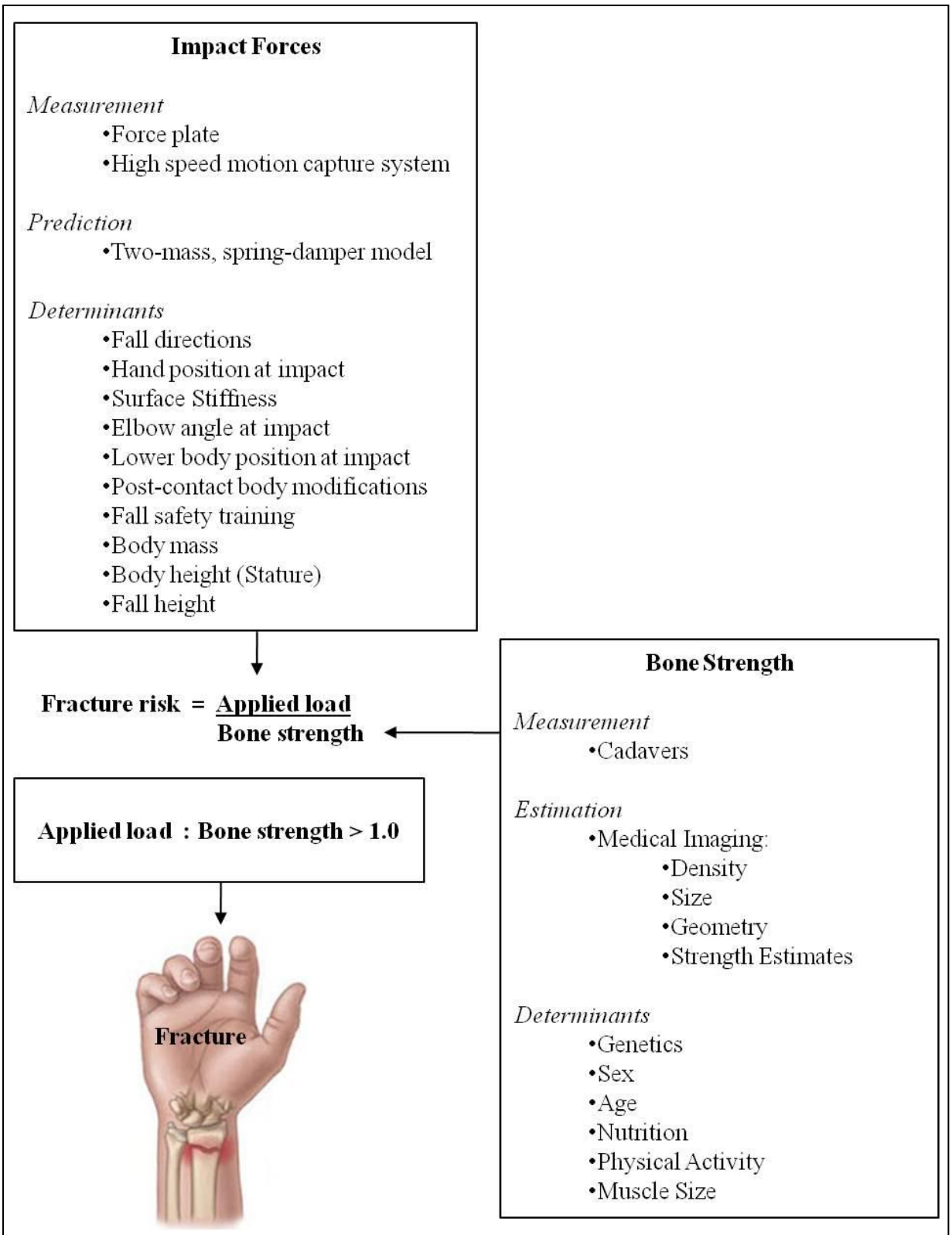

Figure 1. Overview of the fracture risk equation and description of measurement, prediction/estimation, and determinants of forces and bone strength that will be discussed in the literature review.

2.1 Forces: Prediction

My thesis will use a combination of kinetics and kinematics. Briefly, kinetics is the branch of mechanics describing the motion of an object and the applied loads causing that motion (Serway & Jewett Jr., 2004). Impact force refers to the force of the body being applied to the ground at impact. The magnitude of the body's impact force is equal to, but in the opposite direction from, the ground reaction force (GRF) (Serway & Jewett Jr., 2004) (Figure 2). The GRF is the force that can be measured using a force plate and is the force that is applied to the hand of the outstretched forearm. Essentially it is the GRF that will initiate the fracture. I will use the term "force" to refer to the ground reaction force. Kinematics, on the other hand, is the branch of mechanics describing the motion of a particle or rigid body *without* reference to the causes of that motion (Serway & Jewett Jr., 2004). There are six kinematic variables that I will use in this study, they include: position, displacement, velocity, acceleration, time to impact, and elbow joint angle. These variables can be measured using a high speed motion capture system.

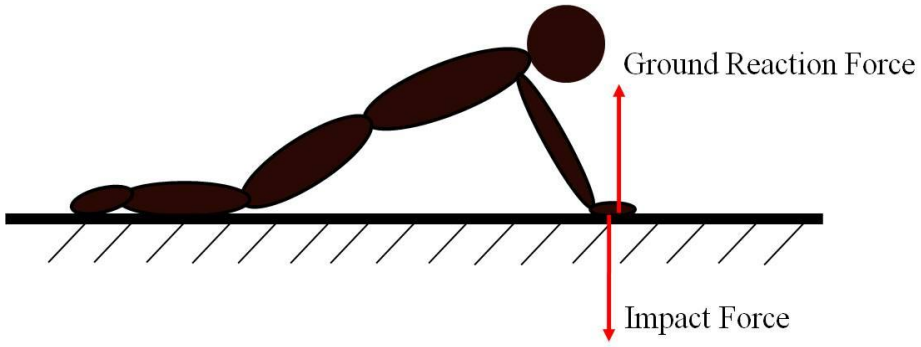

Figure 2. Illustration of the difference between the impact force and the ground reaction force (GRF). The arrows are the same length, but facing opposite directions representing that the impact force and ground reaction force are of equal magnitude but opposite direction.

2.1.3 Mathematical Model and Force Profile

The two-mass, spring-damper model is a mathematical model created in Matlab (2006b, MathWorks, Natick, MS, USA). This model is based on engineering principles, using two

masses connected by springs (stiffness elements: k_s, k_w, and k_g) and dampers (b_s, b_w, and b_g) to recreate the response of the torso and upper extremity during a fall onto the hand of the outstretched forearm (Figure 3a). The mass of the suspended torso is represented by: m_{torso}, and the mass of the arm, that makes the initial contact with the ground: m_{arm}. The mass of the torso is approximately equivalent to 49% of the individual's total body mass (Chiu & Robinovitch, 1998). The mass of the arm has been estimated at 5% of the individual's total body mass (Chiu & Robinovitch, 1998; Clauser, McConville, & Young, 1969).

Within the model, the springs and dampers represent the joints of the upper extremity and the ground (i.e., wrist, *w*, shoulder, *s*, ground (mat), *g*). As in physics, displacing a spring (or joint) results in the production of force in the opposite direction in order to return the spring back to its original position (equilibrium) (Serway & Jewett Jr., 2004). The fundamental equation for the force of a spring is given as:

$$F_s = -kx \quad (1)$$

Where F_s is the force produced in the spring, k is the stiffness constant of the spring, and x is the difference between the springs current length and its resting length (i.e., displacement) (Serway & Jewett Jr., 2004). Stiffness can be defined as generating a spring-like force and is therefore a measure of the joint's resistance to displacement (compression or tensile) (Davidson, Goulding, & Chalmers, 2003; Davidson, Mahar, Chalmers, & Wilson, 2005). Generally speaking, stiff springs have a large k value and do not compress as readily as a spring that is compliant (i.e., having a lower k value) (Martin et al., 1998; Serway & Jewett Jr., 2004). Therefore, an increase in displacement corresponds to an increase in the force produced in the spring. The vertical displacement of the shoulder joint, wrist joint, and ground surface are represented as x_s, x_w, and x_g, respectively. Mathematically, shoulder deflection (i.e., the degree to which an object is displaced) is defined as $(x_s - x_w)$, while wrist deflection is defined as $(x_w - x_g)$.

The damping element is a mechanical element that measures the joint's resistance to velocity, representing the capacity of a mechanical system to dissipate force (Davidson et al., 2003; Davidson et al., 2005; Serway & Jewett Jr., 2004). Damping can be defined as generating a viscous-like force in the opposite direction to the velocity of the system, and is

the reason for the return of the object back to equilibrium (Davidson et al., 2003; Davidson et al., 2005; Serway & Jewett Jr., 2004). The force of the damping element is related to velocity by:

$$F_d = -cv \quad (2)$$

Where F_d, is the force produced in the damper, c is the viscous damping coefficient, and v is the velocity. Therefore, an increase in the velocity of the system corresponds to an increase in the force of the damping element.

These formulae are then combined, based on Newton's second law of motion (*Force = Mass x Acceleration*), and the differential equations are solved using Matlab. The solving of these differential equations is what comprises the model. Given these parameters, the model will predict two peak forces: F_{1max} and F_{2max} (Figure 3b). The first force is a high-frequency transient force (F_{1max}), occurring approximately 20 ms after initial hand contact. F_{1max} is followed by a lower frequency oscillation (F_{2max}), as the rest of the body transmits the force through the arm to the force plate (Chiu & Robinovitch, 1998; Chou et al., 2001; Davidson et al., 2005) (Figure 3b). The second peak has been reported to occur approximately 110 ms after the initial ground impact (Chiu & Robinovitch, 1998).

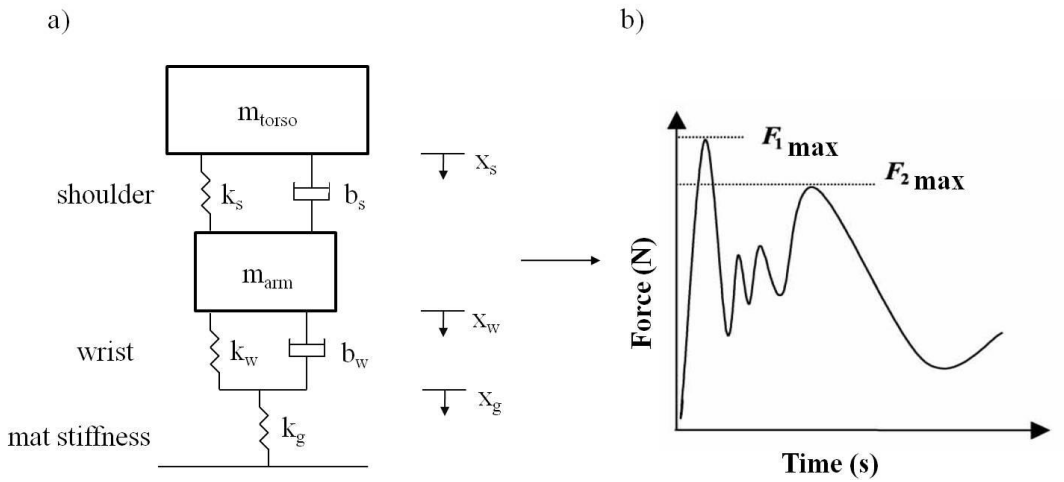

Figure 3. a) Two-mass, spring-damper model was used to simulate the impact response of the body during a forward fall onto the outstretched hand. b) The resultant force profile illustrating that the high-frequency transient force (F_{1max}) occurs shortly after initial hand contact, followed by a lower frequency oscillation (F_{2max}) as the rest of the body transmits energy through the arm to the force plate. Adapted from Robinovitch and Chiu (1998).

2.2 Force Peaks: Determinants

The arm is a kinetic chain, and as such each joint contributes a single part of that chain. At impact on the outstretched arm, the shoulder, elbow, and wrist all work together to provide support for the landing body and act in a way that attenuates the force associated with ground impact. This section will discuss pertinent factors that determine the forces applied to the hand of the outstretched forearm.

2.2.1 Falling Direction

Tan and colleagues investigated the differences in the impact velocities, and thereby resultant forces, between forward and backward falls from standing heights (Tan et al., 2006). Specifically, it was determined that the resultant impact velocity during forward facing falls was 1.33 m/s, which was significantly smaller than those reported during backward falls (2.27 m/s) (Tan et al., 2006). The lower impact velocity associated with forward facing falls corresponds to lower vertical force (F_{1max}) experienced by the hand and wrist at impact. The decreased F_{1max} was explained by the significantly longer force attenuation period during forward facing falls and bending at the elbows upon impact (Tan et al., 2006).

2.2.2 Hand Positioning at Impact

As seen in the falling direction, the hand position during ground impact is also important in altering the magnitude of the force (F_{1max}) applied to the hand at impact. Chou and colleagues (2009) investigated how 3 different forearm rotation angles (i.e., 45^o external rotation, 0^o rotation, and 45^o internal rotation) influenced F_{1max} and elbow flexion angle at impact. They found that external rotation increased F_{1max} on the hand by 1.5 times that of the neutral forearm position, and 2.2 times that of internal rotation (Chou, Lou, Chen, Chiu, & Chou, 2009). Further, in external rotation the elbow remained almost fully extended (3.9^o elbow flexion), relative to the neutral forearm position (24.6^o elbow flexion) and internal rotation (40.3^o elbow flexion) (Chou et al., 2009). These results established that 45^o of external rotation of the hand and forearm leads to a drastic increase in F_{1max} applied to the hand and through the kinetic chain (Chou et al., 2009).

2.2.3 Surface Stiffness

Another force reduction strategy pertains to modifying the surface stiffness. Robinovitch and Chiu (1998) reported that their experiment and simulation (i.e., the two-mass, spring-damper

mathematical model) results supported the notion that falling on compliant surfaces reduced the experimental F_{1max} by an average of 42% (Robinovitch & Chiu, 1998). However, surface stiffness had little effect on F_{2max} and therefore, the force at the shoulder (Robinovitch & Chiu, 1998). This may be attributed to the compliant surface attenuating most of the force at the wrist, thereby delaying peak velocity and reducing F_{1max} (Laing, Tootoonchi, Hume, & Robinovitch, 2006; Laing & Robinovitch, 2009; Robinovitch & Chiu, 1998; Sran & Robinovitch, 2008; Tan et al., 2006). The lack of force attenuation of the compliant surface on F_{2max} may be related to the torso decelerating onto the outstretched arm approximately 90 ms after F_{1max}, and in so doing the force attenuation capacity of the surface has been expended (Robinovitch & Chiu, 1998).

Analyzing surface stiffness has previously been completed for child playground surface stiffness. Most of the research in this area focuses on the comparison between wood fiber surfacing relative to granite sand surfacing. The consensus among all researchers in this area is that granite sand surfacing is more compliant relative to the wood fiber surfacing and thereby attenuates more of the initial impact force (F_{1max}) applied to the hand and wrist (Howard, Macarthur, Rothman, Willan, & Macpherson, 2009; Laforest, Robitaille, Lesage, & Dorval, 2001; Loder, 2008; Sherker & Ozanne-Smith, 2004). These are important findings considering F_{1max} has been associated with fall related injuries (Chiu & Robinovitch, 1998).

2.2.4 Elbow and Shoulder Angle at Impact

The largest forces were reported to transpire when landings occurred on fully outstretched arms (Chou et al., 2009; DeGoede & Ashton-Miller, 2002; Tan et al., 2006). DeGoede and Ashton-Miller (2002) reported that the initial peak force (F_{1max}) and secondary peak force (F_{2max}) were, on average, 40% and 25% lower, respectively, when participant's bent their elbows upon impact (DeGoede & Ashton-Miller, 2002). The decrease in F_{1max} was related to the 11^{o} bend in participant arms during impact. Increasing elbow flexion at impact also resulted in a delayed onset of F_{2max}, allowing the force to be attenuated over increased amount of time (Chou et al., 2001; Chou et al., 2009; Tan et al., 2006). This fall technique not only created a 32% reduction in the peak forces applied to the hands, but also corresponded to a 0.44 m/s reduction in impact velocity at the hands, relative to the torso (DeGoede & Ashton-Miller, 2002). Further, Lo and Ashton-Miller (2008) reported a 10%

reduction in the average wrist impact velocity (from 3.10 m/s to 2.86 m/s, p=0.25) and a 58% reduction in force (from 2212 N to 919 N, p<0.01) when comparing pre-contact shoulder extension and elbow flexion actions to shoulder flexion and elbow extension actions at impact (Lo & Ashton-Miller, 2008).

2.2.5 Lower Body Position at Impact

As previously discussed, conscious control of upper extremity joint movements at impact during a forward fall can significantly reduce the force (F_{1max}) applied to the wrist. However, altering the position of the lower body at impact also significantly reduces force at the wrist (Lo & Ashton-Miller, 2008). Lo and Ashton-Miller (2008) used a computer simulation to investigate the influence of upper and lower body segment alterations on F_{1max} and impact velocity at impact in a forwardly directed fall from standing height. They reported that increased hip extension corresponded to an increase in both F_{1max} and impact velocity attributed to the inability to land on the knees first (Lo & Ashton-Miller, 2008). Therefore, in order to decrease the impact velocity, and thereby the F_{1max}, on the wrist during a forward facing fall from standing height, the hip flexion angle should be greater than 20^{o} so as to allow the first fall related impact to occur on the knees and not the wrist (Lo & Ashton-Miller, 2008).

2.2.6 Post-Contact Body Modification

While it has been established that shifting the body's position at impact can significant reduce F_{1max} and delay the force of F_{2max}, this relationship almost disappears if the action occurs post-contact (Chou et al., 2001; Lo & Ashton-Miller, 2008). Lo and Ashton-Miller (2008) reported that shoulder extension and elbow flexion prior to impact significantly reduce peak wrist force at impact (2212 to 919 N). However, post-impact adjustments of the upper body resulted in increased shoulder flexion and elbow extension. These post-impact adjustments resulted in only minor changes to the wrist forces experienced at impact (1491 to 1078 N). These data suggest that fall injury prevention strategies must be executed prior to ground impact (i.e., during the free-fall phase) in order to decrease the force on the wrist in a forward fall.

2.2.7 Fall Safety Training

Lo and colleagues (2003) investigated whether a 10 minute fall safety intervention would have long term results (i.e., 3 months) in decreasing peak force (F_{1max}). This was tested in young adult males with no previous gymnastics experience or safe fall training. After the brief intervention, there was an 18% reduction in F_{1max} at the hand, relative to baseline (from 880 N to 745 N, $p<0.01$) (Lo, McCabe, DeGoede, Okuizumi, & Ashton-Miller, 2003). At the 3 month testing period, F_{1max} on the hand of the intervention group was still lower than that of the controls (800 N intervention; 813 N controls, $p<0.05$) (Lo et al., 2003). Therefore, the results of this study indicate that fall safety training may decrease F_{1max} at the wrist for at least 3 months post training in young adult males.

2.2.8 Body Mass

Chiu and Robinovitch (1998) reported that increased body mass corresponds to increased magnitude of F_{2max}, while having very little affect on F_{1max}. An explanation is that F_{2max} is the result of the torso negatively accelerating upon the outstretched arm, transmitting the torso mass distally towards the force plate. Thus, an increase in body mass may correspond to an increase in the mass of the torso and thereby an increase in the resultant force applied to the force plate via the outstretched arm.

2.2.9 Body Height (Stature)

Body height (stature) also has a strong and positive correlation to experimental F_{2max} (Chiu & Robinovitch, 1998). However, Chiu and Robinovitch (1998) reported that stature did not correlate with either m_{arm} or m_{torso}, stiffness or damping parameters (Chiu & Robinovitch, 1998). This is surprising considering that increases in stature correspond to increases in body mass (Clauser et al., 1969). However, this lack of relationship was reported to be the result of small sample size (Chiu & Robinovitch, 1998).

2.2.10 Fall Height

The force at impact (F_{1max}) is significantly and positively affected by both experimental and model predicted fall height (Chiu & Robinovitch, 1998; Chou et al., 2001). That is, there is a corresponding increase in F_{1max} as fall height increases. There are other studies investigating impact forces using a free fall drop scenario (Chou et al., 2009; Davidson, Chalmers, & Stephenson, 2006b; DeGoede & Ashton-Miller, 2002; Lo et al., 2003; Lo & Ashton-Miller,

2008). However, their research does not include an investigation into relationship between fall height and the force at impact; thereby limiting the literature to 2 available studies (Chiu & Robinovitch, 1998; Chou et al., 2001).

2.3 Skeletal Strength: Estimated using Medical Imaging

Bone strength can be defined as the ability of the bone to resist fracture, resulting when the ratio of applied load to bone strength is greater than 1.0 (Keaveny & Bouxsein, 2008). Direct measures of bone strength are invasive and require breaking the actual bone, therefore direct measures are only done in cadaveric bones *ex vivo*. Thus, bone strength can only be estimated *in vivo*. Whole bone strength depends on the bone size, geometry (spatial distribution of bone mass), bone mass, and densitometric properties (e.g., cortical or trabecular bone density) (Ammann & Rizzoli, 2003; Bouxsein & Seeman, 2009). These above stated bone properties can be measured using medical imaging techniques.

X-ray based imaging techniques are used to measure the mineral mass and its distribution (i.e., bone structure and geometry) (Petit, Beck, & Kontulainen, 2005). There are three x-ray based medical imaging techniques commonly used to obtain bone parameters: dual-energy x-ray absorptiometry (DXA), computed tomography (CT), and peripheral quantitative computed tomography (pQCT). In the following sections, I briefly introduce how bone strength is estimated using these techniques.

2.3.1 Dual-energy X-ray Absorptiometry

DXA uses low dose radiation x-ray beams from 2 separate sources – one source measures soft tissues, while the other measures bone (Bolotin, 2007; Nielson, 2000). DXA provides a 2-dimensional, projection image of bone variables, such as: bone area, bone mineral density, and bone mineral content. DXA derived, areal bone mineral density (the amount of bone mineral per cross sectional area, aBMD, mg/cm^2), is the most widely used surrogate of bone strength and fracture risk assessment in osteoporotic populations (Griffith, Engelke, & Genant, 2010). However, because DXA provides a planar projection image, it cannot measure cortical and trabecular bone, or define bone geometry (Bolotin, 1998; Bolotin, 2007; Griffith et al., 2010; Nielson, 2000). Researchers consider aBMD to be a poor indicator of individual fracture risk because DXA is unable to assess the structural properties of bone (Augat, Gordon, Lang, Iida, & Genant, 1998; Augat, Iida et al., 1998). However, DXA

continues to be the "gold standard" of clinical bone imaging and fracture risk assessment. Better tools are required to separately measure cortical and trabecular bone and define bone geometry.

2.3.2 Quantitative Computed Tomography

QCT is a densitometric imaging technique used to measure bone size, structure, and density in 3-dimensions, and separately measures cortical and trabecular bone (Njeh, Fuerst, Hans, Blake, & Genant, 1999). QCT is routinely used to determine volumetric bone density the amount of bone mineral per unit volume (vBMD, mg/cm^3), in the spine (Njeh et al., 1999). However, QCT can also be used to accurately and precisely assess densitometric and geometric measures at the distal radius (Engelke et al., 2009). While QCT has been reported to have higher sensitivity relative to DXA in discriminating between women with osteoporosis versus those without, the use of clinical (or helical) QCT exposes the scanned individual to a high amount of radiation (effective dose at forearm: <10 μSV) (Adams, 2009; Engelke et al., 2009). Therefore QCT is used less frequently than DXA (Engelke et al., 2009).

2.3.3 Peripheral Quantitative Computed Tomography

Peripheral QCT is a non-invasive, densitometric imaging technique reported to precisely measure the 3-dimensional volumetric bone density, cross sectional area, and geometry of cortical and trabecular bone of the appendicular skeleton (Riggs et al., 2004; Sievanen et al., 1998). Peripheral QCT derives information from a scan based on the voxels (3-dimensional pixels or cubes) within a defined region of interest. While pQCT measures bone and muscle properties using 3-dimensional voxels, it should be noted that the third dimension (i.e., slice thickness along the z-axis) is a constant 2.3±0.2 mm (Petit et al., 2005). The use of 3-dimensional imaging is beneficial as it takes into account the size difference between patients/participants (Engelke et al., 2009). Further, pQCT has a low effective dose per scan (~0.22 μSv) (Stratec Medisintechnik GmbH, 2004). These features make using pQCT, to measure the forearm bone and muscle structural properties, an attractive alternative to DXA and QCT.

Melton and colleagues (2007) compared pQCT derived bone geometry and strength estimates between women who sustained a fracture and their non-fracture counterparts. They

reported that the distal radius cortical (fracture: 688±65 mg/cm^3; control: 764±107 mg/cm^3; p<0.05), and trabecular (fracture: 115±35 mg/cm^3; control: 147±40 mg/cm^3, p<0.05) volumetric densities were significantly lower in the group who sustained a fracture relative to the non-fracture controls (Melton III et al., 2007). They also reported that the fracture group had significantly lower finite element estimated fracture load (fracture: 2488±521 N; control: 3109±639, p<0.01) (Melton III et al., 2007). Finite element analysis is a mathematically based computational method of breaking a complicated object (i.e., bone) into a finite number of small pieces (i.e., elements) and assigns each piece an appropriate property based on a pre-determined loading condition (Melton III et al., 2007). The results from Melton and colleagues (2007) indicate that a decrease in bone density is associated with decreased bone strength and decreased load applied to fracture the bone.

When a load is applied to bone, the pre-fracture deformation and related stress within the bone tissue are determined by the size and the geometrical arrangement of bone mass (Petit et al., 2005; Seeman & Delmas, 2006). The cross sectional area is used to measure the size of the bone, and can be assessed as total bone area (the area of bone under the periosteum), or separated into cortical and trabecular bone area (Adams, 2009; Petit et al., 2005). Bone geometry is dictated by the spatial distribution of the bone mass around a central or neutral axis (Kontulainen, Hughes, Macdonald, & Johnston, 2007; Martin et al., 1998; Schoenau, Neu, Rauch, & Manz, 2001). Assessing bone size and geometry improves estimations of bone strength because an increase in these properties corresponds to an increase in bone stiffness (i.e., resistance to bending) (Rauch & Schoenau, 2001). Rauch and Schonau (2001) reported that when comparing density measures of a newborn bone to the bone of a 6 month old child, the bone appears to get weaker. However, when the size and geometry of the bone were incorporated into the bone strength assessment, the bone strength actually increased (Rauch & Schoenau, 2001). Therefore, bone size and geometry are valuable assets in determining bone strength.

Bone strength is also dependent on the combination of bone density (Ammann & Rizzoli, 2003; Bouxsein & Seeman, 2009). For instance, an increase in the density (bone mineral content per unit volume, mg/cm^3) corresponds to an increase in the bone stiffness (Bouxsein & Seeman, 2009). Two pQCT derived estimates of bone strength that combine

these strength parameters are bone strength index in compression (BSI_c), and polar strength-strain index (SSI_p).

2.3.3.3 Compressive Bone Strength Index (BSI_c)

At the ends of long bones, the predominant loading type and direction at bone ends is axial compression (Ferretti, Capozza, & Zanchetta, 1996; Hayes & Bouxsein, 1997). The compressive strength of bone, or BSI_c, is proportional to the product of total bone cross sectional area (ToA) and the square of total bone density (ToD^2) (Kontulainen et al., 2008) (Equation 1).

$$BSI_c = ToD^2 \; x \; ToA \tag{3}$$

Bone strength index (BSI_c, mg^2/cm^4) has previously been validated to reflect bone's resistance to compressive loading in the tibia (Kontulainen et al., 2008). At the 4% site, BSI_c predicted 85% ($p<0.05$) of the variance in failure load in the tibia, and 57% ($p<0.05$) of the variance in tibia bone stiffness (Kontulainen et al., 2008). Essentially, BSI_c has been previously reported to be a good predictor of the bone failure load and bone stiffness (degree of bone deformation) in the tibia.

2.3.3.4 Polar Strength Strain Index (SSI_p)

Applying bending and torsional forces are the predominant ways to load the shaft of long bones. The ability of the cortical bone at the shaft to resist stresses from different directions is dependent on the geometrical arrangement and distance of the cortical bone mass from the centroid, or neutral axis, of that bone (Kontulainen et al., 2007; Kontulainen et al., 2008; Martin et al., 1998). SSI_p is a measure of bone's resistance to torsional forces and was highly related ($R^2=0.85$, $p<0.05$) to the radius fracture load (Lochmuller, Lill, Kuhn, Schneider, & Eckstein, 2002; Muller et al., 2003).

$$SSI_p = \sum \frac{\left[(a * \; d^2)\left(\frac{CoD}{ND}\right)\right]}{d_{\max}} \tag{4}$$

In the above equation, *a* is the area of the voxel of interest, *d* is the distance of the voxel of interest from the bone's center of gravity, *CoD* is the volumetric bone mineral

density in the voxel (mg/cm^3), *ND* is the physiological normal density of the bone (set to 1200 mg/cm^3), and d_{max} is the maximum distance, from the bone's center of gravity, of a complete voxel within the cortical cross section (Schoenau et al., 2001) (Figure 4). This algorithm is programmed into the pQCT software.

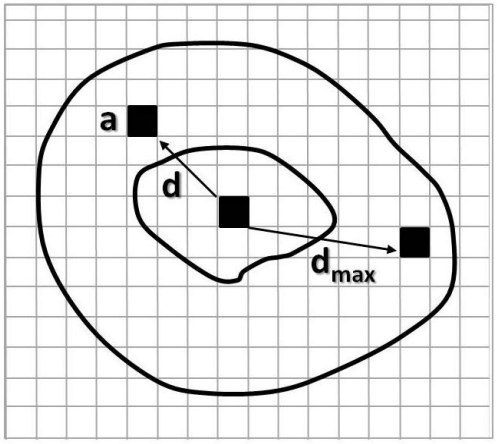

Figure 4. A diagrammatic representation of the cross section of a radius shaft and variables used in calculating polar SSI_p. Grid and black coloured boxes represent the voxels (in this study: 0.4 x 0.4 x 2.3 mm). Modified from Schoenau et al. (2001), and Macdonald et al. (2007).

2.4 Skeletal Strength: Determinants

To optimize fracture prevention, a better understanding of the factors that can deteriorate or enhance skeletal strength is required. There are numerous factors determining bone strength, however, I will briefly discuss the following key determinants: genetics, sex, age, nutrition, physical activity, and muscle strength.

The influence of genetics on bone strength has been estimated to explain 60-80% of the variance in adult aBMD, based on monozygotic and dizygotic twin studies (Bonjour, Chevalley, Ferrari, & Rizzoli, 2009). From puberty onwards, males have more periosteal apposition and endocortical resorption than females, resulting in a larger bone area, increased distance of the bone mass from the neutral axis, and increased bone bending strength (Ferretti et al., 1998; Maynard et al., 1998). Bone porosity and fragility increase with age regardless of sex; however, females tend to sustain fragility fractures earlier in life than males; from a genetics stand point, this is probably resulting from their genetically determined smaller bone

size (Wang & Puram, 2004). Yet, despite the strong association of genetics, sex and age, with bone strength, environmental factors play an important role as they may account for 20-40% of the variance in peak bone strength (Bonjour et al., 2009). For instance, a healthy diet, rich in calcium and vitamin D, is positively and strongly associated with the development and maintenance of bone strength during growth and after menopause, respectively (Seibel, 2007; Vatanparast, Baxter-Jones, Faulkner, Bailey, & Whiting, 2005). Finally, physical activity increases bone strength (Haapasalo et al., 2000). Bone tissue is dynamic, given that the size and geometry of the bone adjusts in order to modify the strength in accordance with the mechanical loads applied to it (Frost, 1987; Petit et al., 2005; Rauch, Bailey, Baxter-Jones, Mirwald, & Faulkner, 2004). For instance, bone size increases with loading, such as physical activity (Haapasalo et al., 2000), and decreases with a lack of loading, such as bed rest, immobilization, or weightlessness associated with space flight (Zhang, Hamamura, & Yokota, 2008). In adulthood, when longitudinal bone growth is completed, an increase in bone length allows for higher force production by the muscle (Turner, 2006). Higher muscle pulling forces on the bone correspond to increased bone strength, through an increase in total and cortical bone area (Ammann & Rizzoli, 2003; Klein, Allman, Marsh, & Rice, 2002; Nikander et al., 2010; Seeman, 2008).

Muscle strength can be defined as the amount of force a muscle can generate (Fukunaga et al., 2001). However, unlike bone, direct measures of muscle strength are easily acquired through the use of hand-grip and isokinetic dynamometry (Frank, Lorbergs, Chilibeck, Farthing, & Kontulainen, 2010; Hasegawa, Schneider, & Reiners, 2001). While the use of dynamometry requires additional testing and may be taxing on the participant, pQCT can be used to calculate muscle cross sectional area (MCSA). MCSA has been shown to be a good surrogate of muscle strength (Frank et al., 2010; Hasegawa et al., 2001).

2.5 Summary of the Literature

In summary, the two-mass, spring-damper model has been validated to predict force peaks (F_{1max} and F_{2max}) up to a fall height of 5 cm. Because of the consistency between the model and experimental data to 5 cm, the model was used to simulate and predict the forces resulting from standing height (0.75 m) falls in the average adult. However, the experimental evidence supporting the accuracy of the model prediction for standing height falls is limited

to low fall heights of 1, 3, and 5 cm (Chiu & Robinovitch, 1998). The relationship of force at impact to fall height for falls from heights greater than 5 cm may not be well represented from 3, low fall heights; consequently, the model predictions may not compare to the experimental forces at higher fall heights. Therefore, safe and higher fall heights are needed to further test the ability of the two-mass, spring-damper model to predict the forces on the hand of the outstretched forearm at higher falling heights.

Previous research has revealed that the amplitude of F_{1max} is positively and strongly associated with fall direction (Tan et al., 2006), impact velocity (Chou et al., 2001), hand position at impact (Chou et al., 2009), hip and knee position at impact (Lo & Ashton-Miller, 2008), fall height (Chiu & Robinovitch, 1998; Chou et al., 2001), and surface stiffness (Chalmers et al., 1996; Howard et al., 2009; Laforest et al., 2001; Laing et al., 2006; Laing & Robinovitch, 2009; Robinovitch & Chiu, 1998). The amplitudes of F_{1max} and F_{2max} are positively and strongly associated with the shoulder and elbow flexion angle at impact (DeGoede & Ashton-Miller, 2002). Unlike F_{1max}, F_{2max} is positively and strongly associated with body mass (Chiu & Robinovitch, 1998; Chou et al., 2001; Davidson et al., 2003), and body height (stature) (Chiu & Robinovitch, 1998). Further, mechanical loads are transmitted to and absorbed within the bone and muscle (Augat, Iida et al., 1998; Augat, Reeb, & Claes, 1996; Chiu & Robinovitch, 1998; Nikander et al., 2006). However, the association between fall related forces ($F_{1max}$and F_{2max}) and bone and muscle strength, as a function of falling height, is unknown. Understanding the factors that predict and determine both forces as well as bone and muscle strength are essential for the optimization of wrist and forearm fracture prevention.

2.6 Objectives

My primary objective is to compare experimentally measured force peaks ($F_{1max\text{-}E}$ and $F_{2max\text{-}E}$) to the force peaks that will be predicted by a simulation model ($F_{1max\text{-}M}$ and $F_{2max\text{-}M}$), at higher fall heights than previously reported (i.e., >5 cm). My second objective is to describe the relationships between the experimentally measured peak forces ($F_{1max\text{-}E}$ and $F_{2max\text{-}E}$) and forearm bone and muscle properties, body mass, and stature as a function of fall height.

3.0 HYPOTHESIS

Regarding my first objective, I hypothesize that the experimentally measured peak forces ($F_{1max\text{-}E}$ and $F_{2max\text{-}E}$) will be comparable to the model simulated forces ($F_{2max\text{-}M}$ and $F_{2max\text{-}M}$) at fall heights higher than 5 cm, when using the generic spring and damping parameters in the model. I hypothesize this because the experimental evidence supporting the model prediction accuracy of standing height falls is limited to low fall heights of 1, 3, and 5 cm. The relationship of force at impact to fall height for falls from heights greater than 5 cm, may not be well represented from 3, low fall heights and consequently, the model predictions may not compare to the experimental forces at higher fall heights..

For my second objective, I hypothesize that $F_{1max\text{-}E}$ and $F_{2max\text{-}E}$ will be correlated to bone and muscle strength estimates, body mass and stature, and that these correlations will increase with increasing fall heights. I hypothesize this because the forces from mechanical loading are transmitted to and absorbed within the bone and muscle (Nikander et al., 2006). Further, based on the premise: *Stress = Force/Area*, an increase in the bone and muscle area would result in a decrease in the stress within the bone and muscle tissues and consequently decrease the risk of fracture (Kontulainen et al., 2008).

4.0 METHODS

4.1 Participants

I recruited a convenient sample of 10 (5 males, 5 females) healthy, right handed adults (mean age 26 ± 4 years) to participate in the study. Participants were not required to be right handed to participate in the study. Recruitment of males to females was done to mimic the recruited participants in Chiu and Robinovitch (1998), to justify the use of the stiffness and damping variables reported from their study (i.e., generic stiffness and damping variables) in the current study. Participants were included into the study if they did not experience an arm or wrist fracture in the past 2 years, if they did not have any bone or other diseases that predisposed them to an increased likelihood of fracture, or if they did not suffered a shoulder or back injury. The maximum capacity of the experimental apparatus is 130 kg, therefore any participant exceeding this mass limitation was excluded. Participant physical activity levels, and nutrition were not considered in this study. These issues were addressed by asking the participants to fill out a short questionnaire prior to their participation in the study (Appendix A). All participants read and signed the consent form prior to participating in the current study (Appendix B). This study was approved by the University of Saskatchewan Biomedical Research Ethics Board (Appendix I).

4.2 Anthropometry

I measured each of the participant's height, without shoes, using a wall mounted stadiometer (Holtain Limited, Crymych, UK) to the nearest 0.1 cm. I also measured each participant's mass, without shoes, on a calibrated electronic scale (Toledo Scale Company, Thunder Bay, Ontario, Canada) to the nearest 0.1 kg.

I estimated the length of the dominant radius by taking the median of three forearm length measures. I measured the length of the forearm from the proximal radiohumeral joint to the distal styloid process of the radius (Norton, Carter, Olds, & Marfell-Jones, 2001).

4.3 Falling Apparatus and Scenario

4.3.1 Apparatus and Harness

The fall-release apparatus was designed and built by the mechanical engineering students as partial fulfillment of their bachelor's degree. The apparatus contains a metal frame with hand

hoist, used to suspend the participant's trunk in to the air. The participant was positioned directly over the force plate, with a 1 cm thick foam mat separating the participant's palm and the force plate (Figure 5). The participants were fitted into an industrial fall restraint harness and suspended in the air via a cable and electromagnet. An electromagnet is a type of magnet where the flow of electric current produces a magnetic field allowing oppositely charged metallic solids to remain in contact with one another. The cessation of the electric current causes the magnetic field to disappear, thereby allowing the metallic solids to break contact with one another. The electromagnet was secured to the steel frame of the fall-release apparatus. Safety chains were attached from the steel frame to the magnet to prevent the released magnet from hitting the participant.

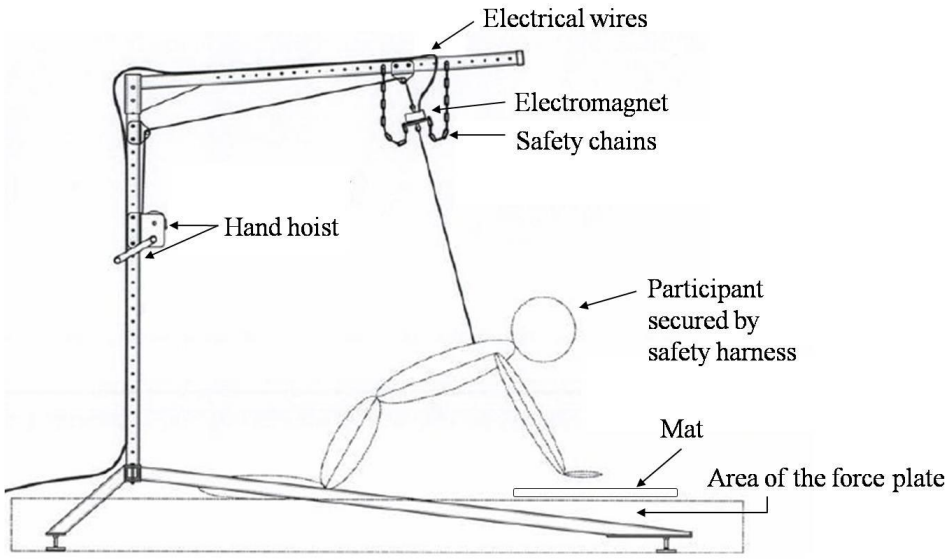

Figure 5. Diagrammatic representation of the fall-release apparatus and fall scenario.

4.3.2 Determination of Fall Height

The fall heights were determined by individually calculating the difference between the participant's hand and the top of a 1cm thick foam mat, that was placed on top of the force plate, using a high speed motion capture system. The following nominal drop heights were used: 1, 3, 5, 7, 10, 15, 20, and 25 cm. The drop heights of 1, 3, and 5 cm were chosen in order to make a comparison between the force data of this study and that reported in Chiu

and Robinovitch (1998) so as to ensure our testing apparatus and procedure were obtaining similar results and increase the generalizability of this study. The incremental drop heights higher than 5 cm were chosen to minimize gaps between force data as a function of fall height. Prior to the study onset, I randomized all fall heights in each of the four fall trials. Therefore, each participant underwent 32 randomized falls.

4.3.3 Body Position

Participants began on their knees, with their shins and the dorsal part of the foot in contact with the ground, holding their forearms and hands outstretched in front of them (Figure 5). The participant's right and left hands were staggered, with the right (dominant) hand directly over the force plate. The rationale for staggering the hands was so that the ground impact would first occur on the dominant hand. Research has indicated that the bones of the dominant limb are stronger than those of the non-dominant limb in athletic and non-athletic populations (Haapasalo et al., 2000; Steele & Mays, 1995). Further, the participant's were instructed to fully extend (outstretch) their elbows during the fall and at impact. Falling with fully extended elbows represents the worst-case falling scenario (Chiu & Robinovitch, 1998). Prior to release of the electromagnet, I checked the body line so that a straight line could be drawn from the knees to the shoulders of the participants (Appendix C). I also instructed all participants to extend their hips into the harness to facilitate proper body line and fall procedure. Finally, I double checked all body position parameters in order to minimize the confounding variables associated with free fall experimentation.

4.3.4 Experimental Protocol

I implemented a single fall type, involving a forwardly directed fall (Figure 5). The electromagnet that suspended the participant's trunk above the force plate was connected to a computer that was programmed to discontinue the flow of current to the electromagnet and in so doing would release the participant into a free fall towards the force plate. Suspension times were programmed into the computer software and ranged from 0.1–5 seconds. The only indication for the cessation of the electrical current, and thereby the release of the participant, was a verbal cue, "ready?".

4.4 Motion Capture Assessment

In order to record the 3-dimensional kinematics, I used an eight camera commercial motion capture system (Vicon Nexus, Vicon Motion Systems, CO). The motion capture system consists of eight high speed motion capture cameras that can track and resolve the 3-dimensional coordinates of the passive reflective markers located on the participant's body. Motion data were captured at 200 Hz.

Twenty-three passive infrared reflective markers (14 mm in diameter) were secured to the participant's skin or clothing by means of clear, hypoallergenic two-sided tape along the right and left sides of the body. More specifically, on the right side, from distal to proximal location, 1 marker was attached to the hand along the third metacarpal, 2 markers were attached to the wrist (radial and ulnar styloid processes), a cluster of 4 markers was attached to the forearm, 2 markers were attached to the elbow (medial and lateral humeral epicondyles), a cluster of 4 markers was attached to the upper arm segment, and 1 marker was attached on the acromion process of the right shoulder. On the left side, from proximal to distal, 1 marker was attached to the wrist (ulnar styloid process), 1 marker was attached to the elbow (lateral humeral epicondyle), and 1 marker was attached on the acromion process of left shoulder. A chest cluster of 4 markers were attached to the participants shirt, just inferior to the sternal notch. Finally, there was 1 marker attached to the left and right lateral femoral condyles (Appendix D).

Eight markers were used for the purpose of calibrating the shoulder joint and then removed post-calibration. Participant shoulder calibration was completed outside of the fall apparatus and prior the fall procedure. Shoulder calibration involved 3 repetitive anterior flexion, 45^{o} flexion, and abduction movements about the right shoulder joint. Shoulder calibration was done to determine the center of the shoulder joint using the movements executed about the shoulder and calculating the pivotal point (Wu et al., 2005). Specifically, calibration markers included the: 2 markers attached to the wrist (radial and ulnar styloid processes), 2 markers attached to the elbow (medial and lateral humeral epicondyles), and the 4 markers comprising the chest cluster.

4.4.1 Motion Capture Data Analysis

The kinematic data were processed in Vicon Nexus and the 3-dimensional marker locations were exported into Matlab (2006b, MathWorks, Natick, MS, USA). Before further analysis, the kinematic data was filtered, in Matlab, using a digital low pass fourth order Butterworth filter, with a cut off frequency of 15 Hz. All passive reflective markers needed to have their relative anatomical position defined and coordinated to the global coordinate system (i.e., that of the motion capture cameras) (Grood & Suntay, 1983; Wu et al., 2005) - this was accomplished using Matlab routines. Using Matlab, I was able to obtain corresponding nominal fall heights, the difference in the elbow joint angles from trial start to impact, time to impact from the start of the trial, and impact velocity. All data, excluding elbow angles, were obtained using the fourth right lower arm marker in the marker cluster. Elbow joint angles were calculated in Matlab as Cardan angle sequences using a floating secondary Cartesian axis (Wu et al., 2005). The elbow joint angle calculations are based on the premise that the humeroulnar joint of the "elbow" is a hinge joint (Wu et al., 2005), and as such I focused my attention to flexion and extension movements. Using Matlab, I was able to determine the motion of the forearm relative to the humerus and thereby determined the difference in the angle of the elbow before the fall and the angle of the elbow at impact. I exported these variables to numerous excel sheets for statistical analysis and comparative graphing purposes.

4.5 Force Assessment

The participants' force was recorded as the force exerted by the participant against the force plate (OR6-7, AMTI, MA). The force plate was embedded in the floor of the data collection platform so that the measuring surface of the force plate is flush with the floor. The force plate is a metal device housing force transducers able to measure the three-dimensional (x, y, z) forces that are applied to the top/measuring surface of the force plate. Force plate data were collected at 2000 Hz.

4.5.1 Force Data Analysis and Outcomes

The kinetic data obtained from the force plate were exported and analyzed by a Matlab routine. I processed the forces in the z-axis, corresponding to the vertical forces applied to the force plate. I determined and labeled the positive inflection point of the resultant force

profile graph (Figure 6), corresponding to the instant the participant's hand made contact with the force plate (i.e., moment of impact). Further, in order to acquire numerical values for the experimental force peaks, I determined $F_{1max\text{-}E}$ and $F_{2max\text{-}E}$ on the force plate outputted force profiles (Figure 6).

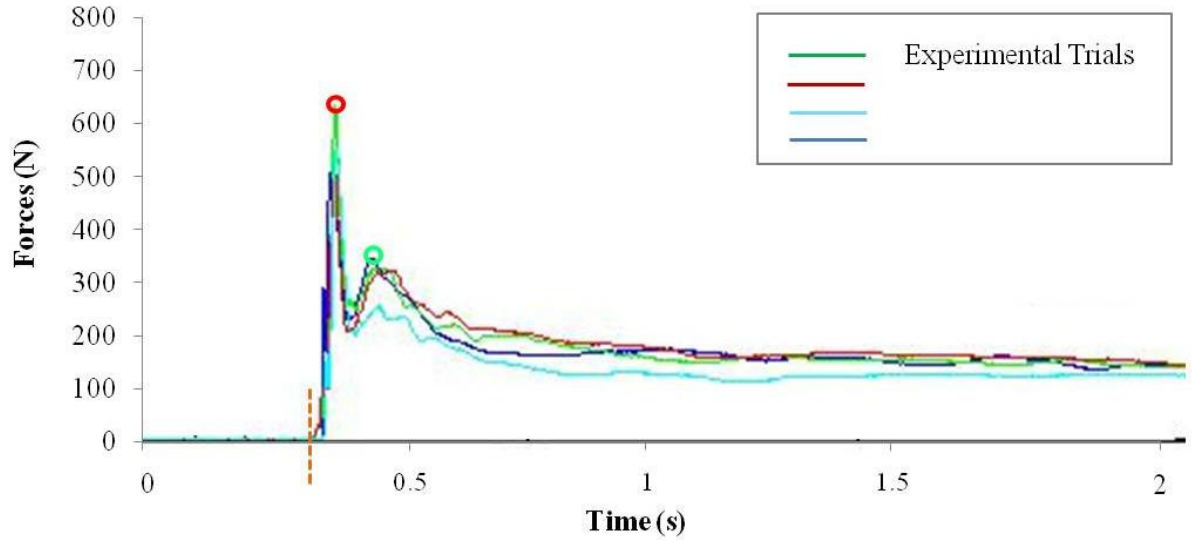

Figure 6. Sample experimental force profile for one participant at one fall height (10 cm), illustrating the positive inflection point (dotted line) and the two peak impact forces: F_{1max} (dark colored circle) and F_{2max} (light colored circle). The forces were filtered using a digital low pass fourth order Butterworth filter, with a cut off frequency of 15 Hz.

4.6 Mathematical Model

The mathematical model was created in Matlab and used to predict the peak forces on the wrist at the moment of impact. The code required by the model was programmed by Devin Glennie and Dr. Joel Lanovaz (PhD). The model was based on the equations of motion below, which have been adapted from Robinovitch and Chiu (1998).

$$m_{arm}\ddot{x}_w + (b_w + b_s)\dot{x}_w + (k_w + k_s)x_w = b_s\dot{x}_s + b_w\dot{x}_g + k_s x_s + k_w x_g + m_{arm}g \quad (5)$$

$$m_{torso}\ddot{x}_s + b_s\dot{x}_s + k_s x_s = b_s\dot{x}_w + k_s x_w + m_{torso}g \quad (6)$$

$$b_w\dot{x}_w + k_w x_w = b_w\dot{x}_g + (k_w + k_g)x_g \quad (7)$$

Where the mass of the torso is represented by: m_{torso}, and the mass of the arm is represented by m_{arm}. The stiffness elements of the shoulder, wrist, and mat (ground) are represented as:

k_s, k_w, and k_g, respectively. The damping elements of the shoulder, wrist, and mat (ground) are represented as: b_s, b_w, and b_g, respectively. The velocity of a given segment (i.e., shoulder, *s;* wrist, *w;* and mat (ground), *g*) is represented by $\dot{x}$, while $\ddot{x}$ is the acceleration of a given segment. The deflection of the mat is defined as x_g. Equations 5-7 were solved using a fourth-order Runge-Kutta numerical integration routine in Matlab. The fourth-order Runge-Kutta is a commonly used higher order integration method for determining the motion of an object over time.

Hand contact force (F_h) is defined by:

$$F_h = k_w(x_w - x_g) + b_w(\dot{x}_w - \dot{x}_g) \tag{8}$$

and shoulder contact forces (F_s) is defined by:

$$F_s = k_s(x_s - x_w) + b_s(\dot{x}_s - \dot{x}_w) \tag{9}$$

Where ($x_w - x_g$) defines wrist deflection, ($x_s - x_w$) defines shoulder deflection. The other model parameters are provided in Table 1.

Table 1. Model parameter values.

Parameter	Overall Average and Standard Deviations
m_{arm} (kg)[1]	3.7
m_{torso} (kg)[2]	41.8
k_w (kN/m)[3]	26.7
k_s (kN/m)[3]	2.8
b_w (kN s/m)[3]	0.67
b_s (kN s/m)[3]	0.29

[1] m_{arm} = 5% total body mass
[2] m_{torso} = 49% total body mass
[3] Data obtained from Chiu and Robinovitch (1998)

4.6.1 Model Data Analysis and Outcomes

I obtained model predicted force data by entering the participant specific mass and participant and trial specific impact velocity into the Matlab model. The model outputted a single force profile for every participant and trial specific impact velocity. Model force profiles were similar to the force profiles obtained experimentally, but without the residual noise associated with experimentation (Figure 7). I determined the model predicted force peaks (i.e., $F_{1max\text{-}M}$ and $F_{2max\text{-}M}$) for every participant at every participant and trial specific impact velocity in order to acquire numerical force data. For ease of understanding, as well as for comparative purposes to Chiu and Robinovitch (1998), I used the participant specific impact velocities at the nominal fall heights. In other words, I used the fall heights that the participant's were dropped from and retrieved the corresponding average impact velocity (from Matlab output data). This procedure allowed me to acquire force data that corresponded to the nominal fall heights. I tabulated and illustrated the participant specific impact velocities, averaged across all trials at every fall height, relative to the nominal fall heights in Appendix E. Fall height can be considered a commonly understood variable, while impact velocity is not. Impact velocity is related to height based on the following equations and scientific principle:

Equation of kinetic energy (*KE*):

$$KE = \frac{1}{2}\, mv^2 \tag{10}$$

Equation of potential energy (*PE*):

$$PE = mgh \tag{11}$$

The Law of Conservation of Energy:

$$mgh_o + \frac{1}{2}mv_o^2 = mgh_f + \frac{1}{2}mv_f^2 \tag{12}$$

The law of conservation of energy states that energy can neither be created nor destroyed, only transferred from one form to another (Serway & Jewett Jr., 2004); in this case, energy was transferred from potential energy to kinetic energy. The kinetic energy at the onset of the trial was zero because there is no velocity, and the potential energy at impact was zero

because the height is zero. The relationship between impact velocity and height can further be illustrated combining equations 10-12:

$$mgh_o = \frac{1}{2}mv_f^2$$

$$gh_o = \frac{1}{2}v_f^2$$

$$v_f = \sqrt{2gh_o} \quad (13)$$

Where m represents the mass of the participant. Mass was a common element of both equation and was cancelled out. The variables at the start of the trial were: v_o, representing the initial velocity (which is zero), and h_o representing the initial height (i.e., 1, 3, 5, 7, 10, 15, 20, 25). Gravity, g, is a constant 9.81 m/s^2. The final velocity, v_f, is the velocity at impact when falling from a height of h_o.

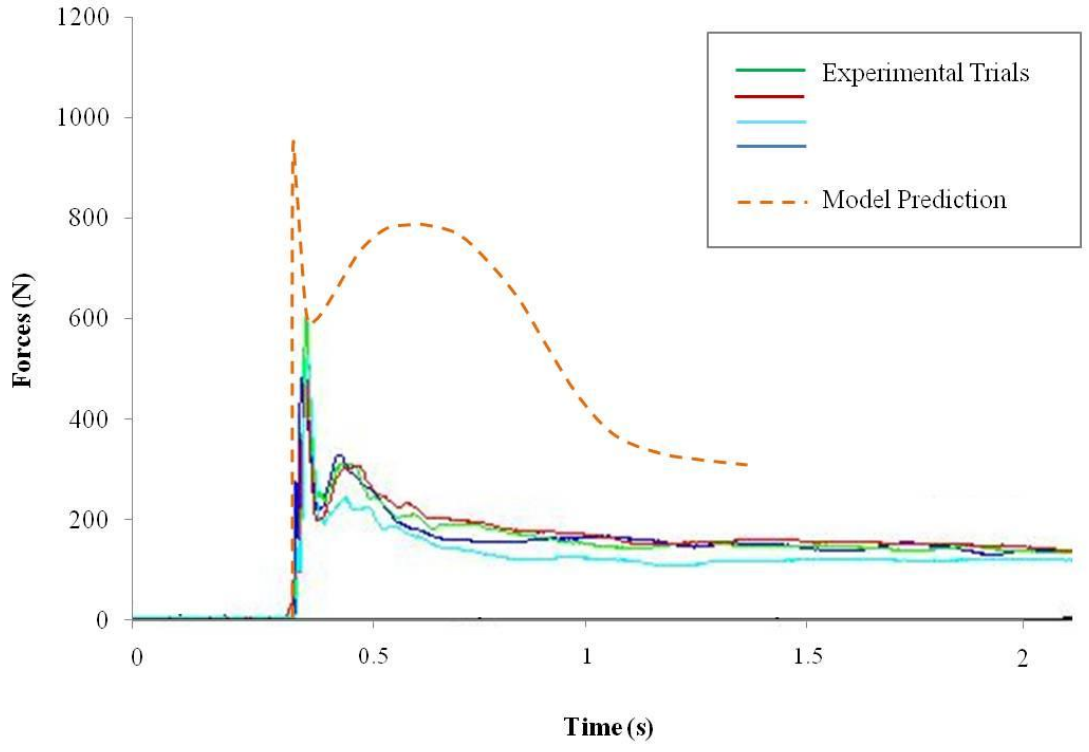

Figure 7. Illustration of the difference between experimental trials (solid colored lines) and the model prediction (orange dotted line) for one participant at one specific fall height. Note that this figure represents raw data and illustrates that there were four trials per fall height.

4.7 Bone and Muscle Strength Assessment

I measured the radius of the dominant arm at 4% and 65% of forearm length from the medial tip of the distal radius end plate (determined by a scout scan) with pQCT (XCT 2000, Stratec GmbH Pforzheim, Germany) (Figure 8). I obtained a 2.4 mm slice at the wrist and radial shaft using a resolution of 400 μm (0.4 x 0.4 mm). I set the scanning speed to 20mm/s. One projection block was used. The scanning protocol is described further in Appendix F. The 4% site was chosen to estimate bone strength at a clinically relevant location prone to fracture, while the 65% site represents the skeletal site with only cortical bone and the largest muscle cross sectional area (MCSA) (a surrogate for muscle strength) (Frank et al., 2010; Hasegawa et al., 2001). The radiation dose (<1 μSv) that the participants' were exposed to was less than the estimated average natural background radiation for which North Americans are exposed to annually (3.0 mSv) (National Council on Radiation Protection and Measurements (NCRP), 2009).

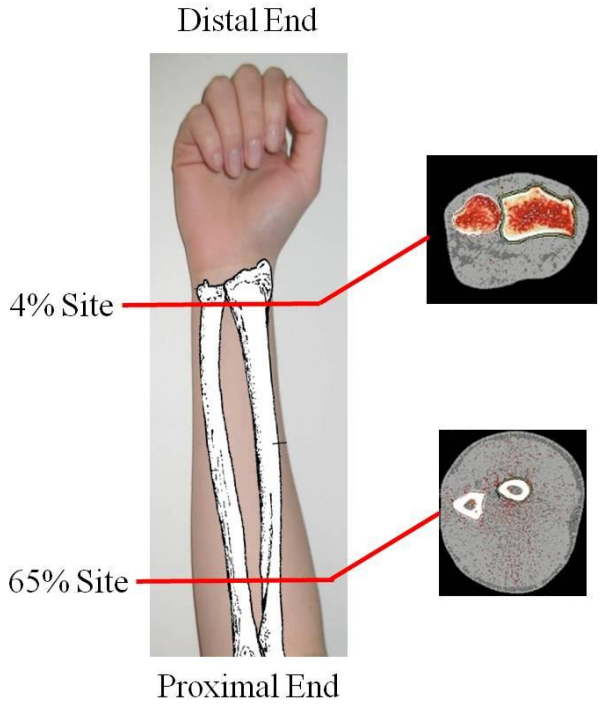

Figure 8. Diagrammatic representation of the 4% (distal) and 65% (proximal) pQCT scanning sites of the right forearm (left) with examples of resultant images (right)

4.7.1 pQCT Data Analysis and Outcomes

I analyzed all scans using Stratec software (version 6.00). Specifically, I analyzed the distal 4% site scans to acquire the total bone area (ToA, mm^2) and density (ToD. mg/cm^3). At the 65% site, I analyzed the scans to yield cortical bone density (CoD, mg/cm^3). I calculated the estimates of radius bone strength at the distal and shaft sites. At the distal site I calculated compressive bone strength index (BSI_c, mg^2/cm^4), using equation 1: $BSI_c = ToD^2 \times ToA$ (Kontulainen et al., 2008). At the shaft, I obtained the polar stress strain index (SSI_p, mm^3), which was calculated from cortical bone by pQCT software. I calculated MCSA by subtracting the total radius and ulna cross sectional areas from the total limb cross sectional area at the 65% site.

I analyzed all pQCT scans of the 4% radius using Contour mode 1, with a threshold of 280 mg/cm^3, in order to define the total bone area (Stratec Medisintechnik GmbH, 2004). I defined the trabecular region using Peel mode 2, with a threshold of 480 mg/cm^3. For the 65% site of the radius, I determined the cortical bone density and area using Separation mode 4, setting the outer cortical threshold to 280 mg/cm^3 and the inner threshold to 480 mg/cm^3. For the muscle analysis at the 65% site, I determined the total limb area using Contour mode 1, with an outer threshold of 40 mg/cm^3.

4.8 Statistical Analysis

Descriptive Data

I analyzed the data to attain the mean and standard deviation (SD) for age, stature, and body mass. Further, I report descriptive data for bone parameters at the 4 and 65% scan sites, and muscle parameters at the 65% scan site. Normal distribution of data was determined by dividing the skewness and kurtosis values to their corresponding standard error values (Vincent, 2005).

Forces: Experimental Outcomes versus Model Predictions

I performed two 2x8 between-within factorial analysis of variance (ANOVA) tests to compare the forces (F_{1max} and F_{2max}) between the experiment and model across all 8 fall heights. I pooled the genders for all statistical analyses. Further, I controlled for participant mass by dividing each experimental and model force output by the corresponding participant

specific body mass. The first ANOVA was used to determine the difference between $F_{1max\text{-}E}$ and $F_{1max\text{-}M}$ at all fall heights. The second ANOVA was used to determine the difference between $F_{2max\text{-}E}$ and $F_{2max\text{-}M}$ at all fall heights. I performed post hoc analyses using dependent samples *t*-tests at all experimental fall heights. To prevent Type I error the significance value was adjusted by dividing the alpha value of 0.05 by the number of dependent samples *t*-test I used (i.e., 8; therefore 0.05/8 = 0.0063).

Relationship Between Bone and Muscle Strength Estimates and Forces

I performed two Pearson's bivariate correlation tests, pooling the genders, to determine the relationship among forces and participant bone, muscle, and body size (body mass and stature) parameters, at all fall heights. The first correlation test was used to assess the relationship among the $F_{1max\text{-}E}$ and participant MCSA, bone strength index (BSI_c), strength-strain index (SSI_p), body mass, and stature. The second correlation test was used to determine the relationship among the $F_{2max\text{-}E}$ and participant MCSA, BSI_c, SSI_p, body mass, and stature. I squared the correlation values to obtain the coefficient of determination among MCSA, BSI_c, SSI_p, body mass, stature and the experimental force peaks ($F_{1max\text{-}E}$ and $F_{2max\text{-}E}$) at all fall heights.

In order to describe the relationship between the force peaks and the bone and muscle strength estimates, I controlled the forces for mass. In order to control the forces for body mass, I divided each of the forces by their corresponding participant specific body mass (kg). I subsequently performed two more Pearson's bivariate correlation tests. Significance was accepted at $\alpha = 0.05$.

5.0 RESULTS

5.1 Descriptive Data

All 10 participants satisfied the inclusion criteria. Males (n=5) and females (n=5) were combined for statistical analyses. An overview of the participant's average (SD) descriptive variables combining sex are presented in Table 2. The mass of the harness was measured to be 3.7 kg. The average (SD) site-specific bone and muscle variables are presented in Table 3. I have also created additional tables illustrating participant specific descriptive variables (Appendix G). All data were normally distributed. All data were considered to be normally distributed.

Table 2. Descriptive variables of all participants, presented as average (± standard deviation, SD).

Variables	**Average (n = 10)**
Age (years)	26 ± 4
Stature (cm)	169.5 ± 9.5
Mass (kg)	74.0 ± 14.3
Mass with Harness (kg)	77.7 ± 14.3
Mass of torso with Harness (kg)	40.0 ± 7.0
Mass of arm (kg)	3.7 ± 0.7

Table 3. Average (± SD) bone and muscle variables at the 4% and 65% scan sites.

Variables	**Average (n = 10)**
Bone - 4% Site	
Total Area (ToA, mm^2)	416.54 ± 101.09
Total Density (ToD, mg/cm^3)	359.04 ± 34.15
Bone Strength Index (BSI_c, mg^2/cm^4)	54.78 ± 19.84
Bone - 65% Site	
Cortical Area (CoA, mm^2)	132.51 ± 27.97
Cortical Density (CoD, mg/cm^3)	895.39 ± 65.3
Strength Strain Index (SSI_p, mm^3)	350.66 ± 113.36
Muscle - 65% Site	
Total Area (ToA, mm^2)	4781.17 ± 1566.10
Muscle Cross Sectional Area (MCSA, mm^2)	4632.45 ± 1535.84

5.2 Forces: Experimental Outcomes versus Model Predictions

F_{1max} and F_{2max}: Experimental versus Model

There was no significant difference in the first mass controlled force between the experimental ($F_{1max\text{-}E}$) and model ($F_{1max\text{-}M}$) across all fall heights, ($F(7,144)=2.080$, $p=0.079$) (Figure 9a). However, mass controlled $F_{2max\text{-}E}$ and $F_{2max\text{-}M}$ differed across all fall heights, ($F(7,144)=9.961$, $p<0.001$) (Figure 9b). Further, $F_{2max\text{-}E}$ stayed relatively constant (i.e., mean range: 5.15 – 6.62 N/kg; mean difference: 1.37 N/kg) as the fall heights increased, while $F_{1max\text{-}M}$ increased steeply with increasing fall heights (i.e., mean range: 4.33 – 13.86 N/kg; mean difference: 9.53 N/kg). Post hoc analysis identified that $F_{2max\text{-}E}$ and $F_{2max\text{-}M}$ significantly differed at all tested fall heights: $t(9)_{1cm}=6.619$, $p<0.001$, $t(9)_{3cm}=6.206$, $p<0.001$, $t(9)_{5cm}=7.715$, $p<0.001$, $t(9)_{7cm}=8.638$, $p<0.001$, $t(9)_{10cm}=13.649$, $p<0.001$, $t(9)_{15cm}=10.737$, $p<0.001$, $t(9)_{20cm}=8.858$, $p<0.001$, $t(9)_{25cm}=10.160$, $p<0.001$.

I report participant specific, mass controlled: $F_{1max\text{-}E}$, $F_{2max\text{-}E}$, $F_{1max\text{-}M}$, and $F_{2max\text{-}M}$ in Appendix J. Figure 9 *a* and *b* (below) graphically illustrate the mean force recorded at each fall height, averaged with all participants force plot (±SD) at each nominal fall height. I also report participant specific elbow angle differences from the start of the fall trial to impact in Appendix H. Further time to impact can be found in Appendix I.

a)

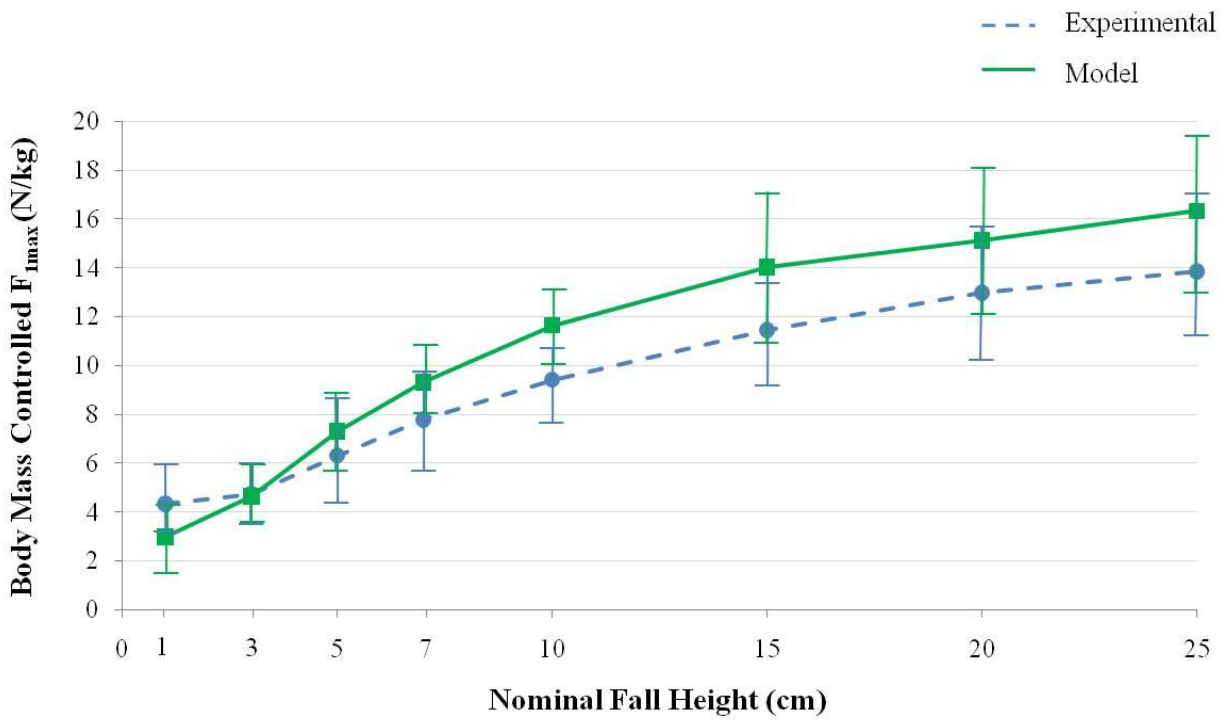

b)

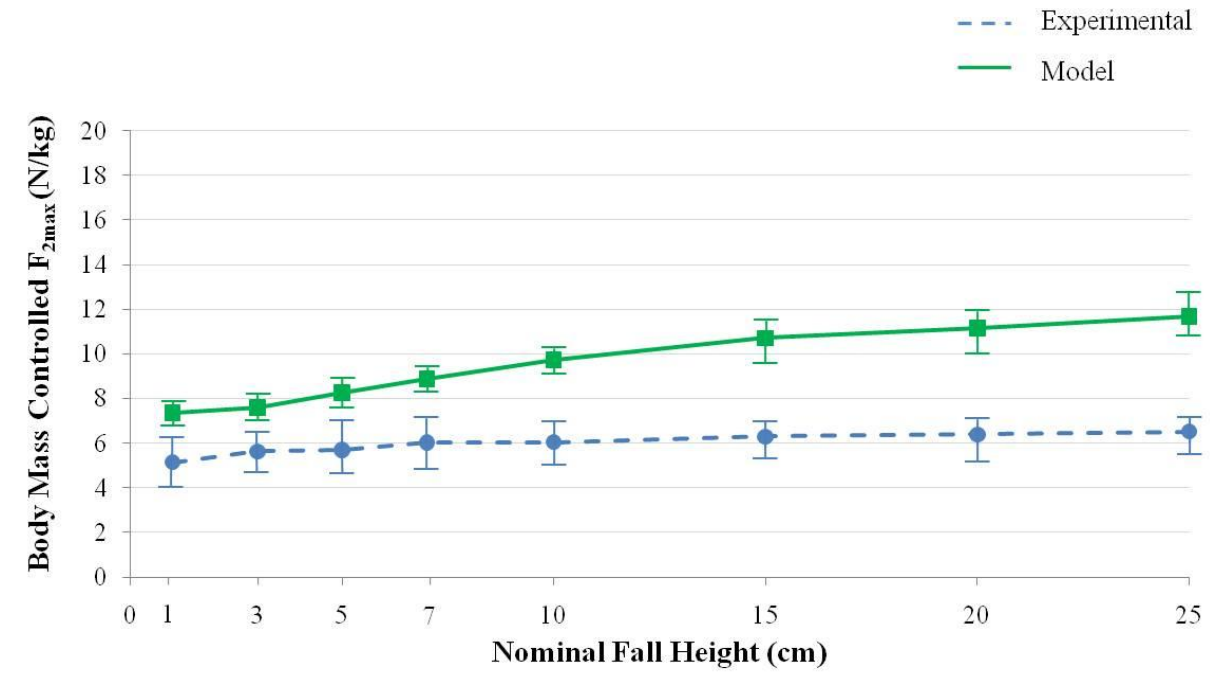

Figure 9. Graphical comparison of a) F_{1max} and b) F_{2max} between the mean experimental (±SD) (blue dotted line) and mean model (±SD) (green solid line) fall scenarios across all fall 8 tested fall heights.

5.3 Relationship Between Bone and Muscle Strength Estimates and Forces

Body mass is highly correlated with bone and muscle strength estimates (MSCA, BSI_c, and SSI_p) (Table 4). This high correlation among body mass and the bone and muscle strength estimates (BSI_c and SSI_p) is the justification of adding mass controlled analyses to this study.

Table 4. Pearson's bivariate correlation matrix among MCSA (mm^2), body mass (kg), BSI_c (mg^2/cm^4), and SSI_p (mm^3) for all pooled participants.

		MCSA	**Body Mass**	**BSI_c**	**SSI_p**
MCSA	*Pearson Correlation*	1	0.913**	0.839**	0.905**
	Sig. (2-tailed)		0.000	0.002	0.000
Body Mass	*Pearson Correlation*	0.913**	1	0.728*	0.804**
	Sig. (2-tailed)	0.000		0.017	0.005
BSI_c	*Pearson Correlation*	0.839**	0.728*	1	0.934**
	Sig. (2-tailed)	0.002	0.017		0.000
SSI_p	*Pearson Correlation*	0.905**	0.804**	0.934**	1
	Sig. (2-tailed)	0.000	0.005	0.000	

* Correlation is significant at the 0.05 level (2-tailed).

** Correlation is significant at the 0.01 level (2-tailed).

Pearson's bivariate correlations for both $F_{1max\text{-}E}$ and $F_{2max\text{-}E}$ to body mass were significant at all fall heights (Table 5 and Table 7). Pearson's bivariate correlations for $F_{2max\text{-}E}$ and MCSA, BSI_c, SSI_p, body mass, and stature were significant at all fall heights (Table 7). However, the strong and statistically significant correlations of F_{1max} and F_{2max} to MCSA, BSI_c and SSI_p disappeared when body mass was accounted for (Table 6 and Table 8). All correlations were positive and seemed to increase with increasing fall height greater than 5 cm.

Table 5. Pearson's Bivariate Correlations for F_{1max-E}

Nominal Fall Height (cm)	MCSA (mm^2)	BSI_c (mg^2/cm^4)	SSI_p (mm^3)	Body Mass (kg)	Stature (cm)
1	0.601	0.581	0.621	0.831*	0.601
3	0.711*	0.648*	0.682*	0.882*	0.756*
5	0.577*	0.405	0.556	0.701*	0.631
7	0.736*	0.558	0.682*	0.807*	0.795*
10	0.845*	0.735*	0.788*	0.871*	0.855*
15	0.878*	0.764*	0.809*	0.863*	0.813*
20	0.837*	0.677*	0.701*	0.831*	0.718*
25	0.870*	0.696*	0.749*	0.719*	0.751*

* Correlation is significant at the 0.05 level (2-tailed).

Table 6. Pearson's Bivariate Correlations for Body Mass Controlled F_{1max-E}

Nominal Fall Height (cm)	MCSA (mm^2)	BSI_c (mg^2/cm^4)	SSI_p (mm^3)	Stature (cm)
1	0.291	0.321	0.357	0.363
3	0.374	0.386	0.421	0.544
5	0.271	0.152	0.318	0.405
7	0.417	0.290	0.443	0.591
10	0.474	0.494	0.543	0.613
15	0.598	0.588	0.624	0.574
20	0.557	0.464	0.458	0.419
25	0.426	0.371	0.378	0.307

Table 7. Pearson's Bivariate Correlations for F_{2max-E}

Nominal Fall Height (cm)	**MCSA (mm^2)**	**BSI_c (mg^2/cm^4)**	**SSI_p (mm^3)**	**Body Mass (kg)**	**Stature (cm)**
1	0.843*	0.770*	0.791*	0.794*	0.713*
3	0.784*	0.850*	0.846*	0.838*	0.720*
5	0.713*	0.714*	0.762*	0.792*	0.674*
7	0.774*	0.713*	0.783*	0.852*	0.731*
10	0.800*	0.764*	0.807*	0.854*	0.732*
15	0.884*	0.861*	0.917*	0.880*	0.877*
20	0.835*	0.917*	0.932*	0.828*	0.798*
25	0.870*	0.900*	0.910*	0.884*	0.817*

* Correlation is significant at the 0.05 level (2-tailed).

Table 8. Pearson's Bivariate Correlations for Body Mass Controlled F_{2max-E}

Nominal Fall Height (cm)	**MCSA (mm^2)**	**BSI (mg^2/cm^4)**	**SSI (mm^3)**	**Height (cm)**
1	0.441	0.501	0.490	0.316
3	0.347	0.659	0.596	0.343
5	0.309	0.459	0.479	0.302
7	0.439	0.485	0.542	0.418
10	0.290	0.482	0.480	0.291
15	0.275	0.531	0.545	0.398
20	0.137	0.542	0.476	0.189
25	0.198	0.586	0.497	0.228

Body mass appeared to have a tendency towards having a stronger relationship with $F_{1max\text{-}E}$ at fall heights under 15 cm (Figure 10a). Interestingly, after fall heights of 15 cm MCSA appeared to have a tendency towards having a stronger relationship with $F_{1max\text{-}E}$ (Figure 10a) and this relationship appeared to remain after controlling for mass (Figure 10b).

a)

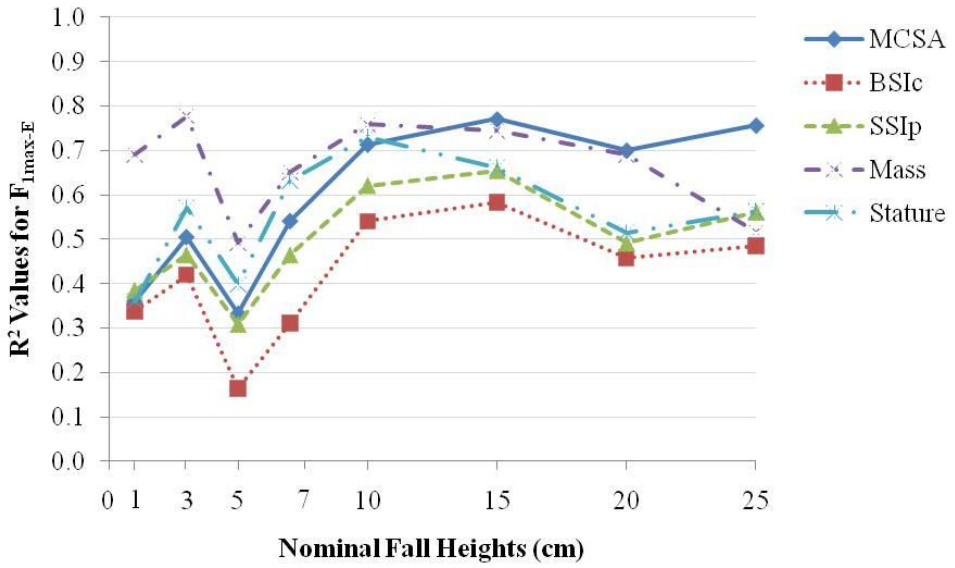

b)

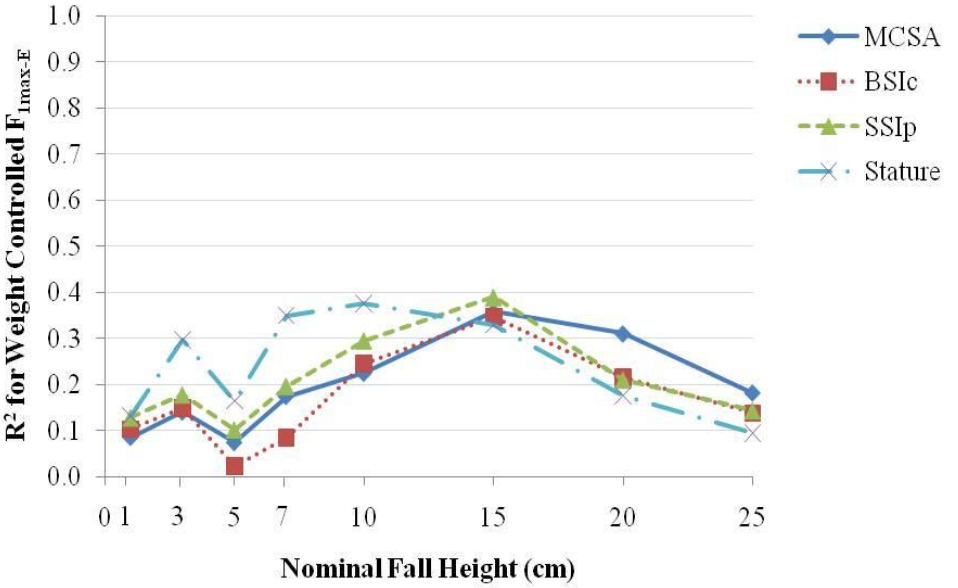

Figure 10. Variance in a) $F_{1max\text{-}E}$ and b) weight controlled $F_{1max\text{-}E}$, accounted for by muscle cross sectional area (MCSA), bone strength index (BSI_c), strength-strain index (SSI_p), body mass, and stature.

Consistent with previous research (Chiu & Robinovitch, 1998), Figure 11a illustrates that body mass appeared to have a tendency towards having a stronger relationship with $F_{2max\text{-}E}$ at fall heights lower than 15 cm. After 15 cm, however, BSI_c and SSI_p appeared to have a tendency towards having a stronger relationship with $F_{2max\text{-}E}$. Interestingly, this relationship is present after controlling for body mass (Figure 11b).

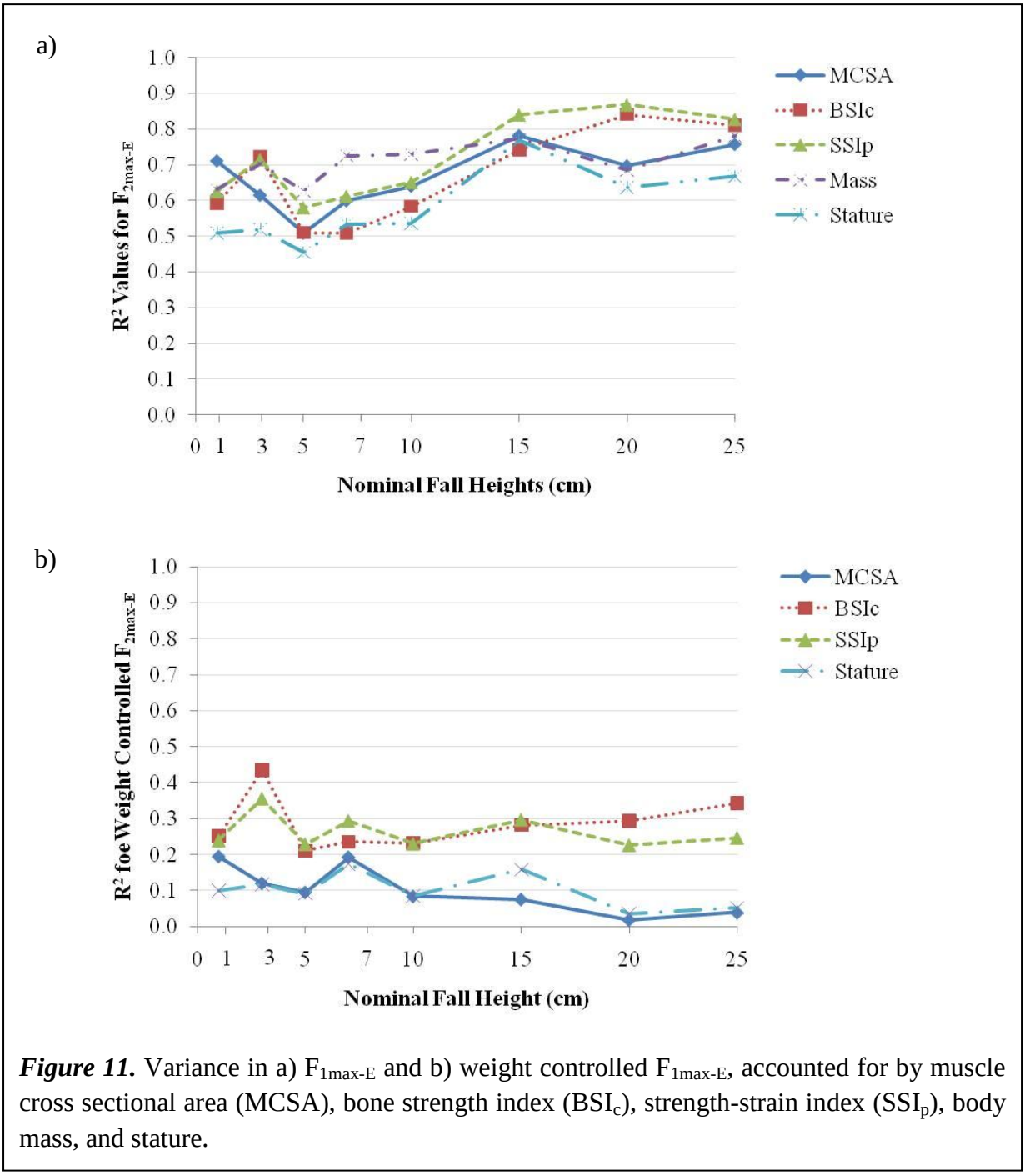

Figure 11. Variance in a) $F_{1max\text{-}E}$ and b) weight controlled $F_{1max\text{-}E}$, accounted for by muscle cross sectional area (MCSA), bone strength index (BSI_c), strength-strain index (SSI_p), body mass, and stature.

6.0 DISCUSSION AND CONCLUSION

6.1 Discussion

Forces: Experimental Outcomes versus Model Predictions

My primary objective was to compare experimentally measured force peaks ($F_{1max\text{-}E}$ and $F_{2max\text{-}E}$) to the force peaks that were predicted by the simulation model ($F_{1max\text{-}M}$ and $F_{2max\text{-}M}$), at fall heights higher than 5 cm. I recollected data at 1 and 3 cm as well so as to be able to compare experimental force outputs with Chiu and Robinovitch (1998). My results revealed that $F_{1max\text{-}E}$ did not significantly differ from $F_{1max\text{-}M}$, when using generic stiffness and damping parameters, across all fall heights. This finding was consistent with previous research (Chiu & Robinovitch, 1998). Although Chiu and Robinovitch (1998) inittially reported that their model under-predicted $F_{1max\text{-}E}$, they adjusted the wrist damping variable in the model to match $F_{1max\text{-}M}$ with $F_{1max\text{-}E}$ (Chiu & Robinovitch, 1998). These were the damping parameters that I used in the current study. Unlike F_{1max}, however, there was a significant difference between $F_{2max\text{-}E}$ and $F_{2max\text{-}M}$. My results revealed that the model significantly over-predicted $F_{2max\text{-}E}$ across all fall heights. This finding was also consistent with Chiu and Robinovitch (1998). However, in order to attain congruency between the experiment and model outcomes, they adjusted the shoulder stiffness variable so the $F_{2max\text{-}M}$ would yield data within ±5% of the $F_{2max\text{-}E}$ (Chiu & Robinovitch, 1998). While I used these stiffness variables in this current study, I did obtain $F_{2max\text{-}E}$ and $F_{2max\text{-}M}$ results that were significantly different from one another.

One possible explanation for the inconsistency between $F_{2max\text{-}E}$ and $F_{2max\text{-}M}$ in this study, may reside in the use of generic stiffness parameters for the shoulder. For instance, the generic shoulder stiffness value may have resulting in the model predicting a stiffer shoulder than what occurred with our participants. However, Chiu and Robinovitch reported that the shoulder stiffness variable decreased with increasing fall height (Chiu & Robinovitch, 1998). Therefore, a more likely explanation of the over-prediction of $F_{2max\text{-}E}$ by the model is that our participant's had more elbow flexion at impact, while the model predicted landings with straightened elbows (Appendix H). As indicated from my results, an increase in elbow flexion at impact as the fall height increased may have lead to increased discrepancy between the model and experimental data as fall height increased. It has previously been established

that the magnitude of the forces is lower as the elbow flexion angle increases (DeGoede & Ashton-Miller, 2002). The increase in elbow flexion angle corresponds to a decrease in the stiffness of the arm segment and a decrease in the impact velocity generated across the wrist (DeGoede & Ashton-Miller, 2002; Robinovitch & Chiu, 1998). Chiu and Robinovitch (1998) did not report their elbow flexion angles, therefore this assumption cannot be confirmed without optimizing our model stiffness and damping elements and comparing these variables to those reported in Chiu and Robinovitch (1998).

Regardless, the model was able to predict the experimental impact forces up to 25 cm of falling height. The magnitude of F_{1max} has been the focus of discussion in previous literature as it exceeds F_{2max} for all fall heights greater than 3 cm (Chiu & Robinovitch, 1998; Davidson et al., 2003; DeGoede & Ashton-Miller, 2002; Lo et al., 2003; Lo & Ashton-Miller, 2008; Robinovitch & Chiu, 1998; Tan et al., 2006). Consequently, F_{1max} has been reported to be the predominant force for the prediction of fracture risk when falling onto the hand of the outstretched forearm (Chiu & Robinovitch, 1998). With these details in mind, it would be feasible to use the two-mass, spring-damper model, with the generic stiffness and damping elements, to predict participant specific forces at impact when falling forward from standing height on to outstretched arms. The information acquired using this model could then be entered as the numerator of the fracture risk prediction equation illustrated in Figure 1. There is controversy in the literature pertaining to what factor should be entered into the numerator and denominator. For instance, Melton et al (2007) and MacNeil and Boyd (2008)used an imaging based finite element analysis to represent bone strength (the denominator of the fracture risk equation), while Ural (2009) used finite element analysis as a representation of the applied load (the numerator of the fracture risk equation. Further research in this area is required in order to clarify this discrepancy within the literature and before this equation can be used in a clinical setting.

Relationship Between Bone and Muscle Strength Estimates and Forces

The second objective of this study was to investigate the relationships between the experimentally measured peak forces ($F_{1max\text{-}E}$ and $F_{2max\text{-}E}$) and forearm bone and muscle properties, body mass, and stature as a function of fall height. I was particularly interested in describing whether estimates of muscle and bone strength would provide more predictive

capacity of fall related forces on the hand of the outstretched forearm over and above that of body mass. I found significant moderate and positive correlations (r_{range}=0.6-0.9, p>0.05) between F_{1max-E} and BSI_c, SSI_p, MCSA, body mass, and stature. Further, the correlations between F_{1max-E} and BSI_c, SSI_p, MCSA, body mass, stature appeared to increase on average by 32%, 25%, 43%, 3%, and 16%, respectively, between 5 and 25 cm; however, these were found when I did not control F_{1max-E} for mass. After accounting for body mass, these large percent increases disappear. For instance, after controlling for mass, the correlations between F_{1max-E} and BSI_c, SSI_p, and MCSA increase on average by 3.5%, 1.6%, and 9.6%. Stature, on the other hand, actually decreases on average by 3.8%, when accounting for body mass. These results establish the strong connection of BSI_c, SSI_p, and MCSA to body mass.

The increasing relationship between the forces and bone and muscle strength estimates, as a function of fall height, warrants some discussion; specifically, the increases in the relationship among F_{1max-E} and MCSA, BSI_c, SSI_p, respectively. The damping coefficient of the arm segment has previously been shown to increase with increasing muscle force while performing isometric contractions (Zhang & Rymer, 1997). Further, it has been established that the stiffness and damping coefficients at the wrist increase with muscle activation and velocity (i.e., rate of change in the joint's displacement) (Milner & Cloutier, 1998). My results are consistent with previous literature as the association between bone and muscle strength estimates and force peaks seem to become stronger with increasing fall height. However, from 20 to 25 cm there appeared to be a slight increase in the relationship between F_{1max-E} and MCSA (r_{20cm}=0.56 and r_{25}=0.43, p>0.05), relative to BSI_c (r_{20cm}=0.46 and r_{25}=0.37, p>0.05), SSI_p (r_{20cm}=0.54 and r_{25}=0.38, p>0.05), and stature (r_{20cm}=0.41 and r_{25}=0.31, p<0.05). This strong relationship between F_{1max-E} and MCSA is not significant after accounting for body mass. This relationship may be a result of the drop protocol used in this study. Further research should compare this study with one employing a bent arm protocol to confirm this speculation. However, this relationship may also be the result of increased muscle contraction with increasing fall height, thereby causing an increase in the stiffness of the system and ultimately increased F_{1max-E} (Chiu & Robinovitch, 1998; Milner, 2002). A natural adaptation to increasing the energy applied to the kinetic chain (e.g., increasing fall height) is to increase the stiffness of the system through co-contraction of extensor and flexor muscle groups around a joint (Milner & Cloutier, 1998; Milner, 2002). My results are

consistent with this statement because the elbow flexion angle was lower as fall heights increased (Appendix H), this may indicate a co-contraction of the biceps and triceps across the elbow, as well as the flexors and extensors across the wrist. However, electromyography (EMG) data is needed to confirm this assumption.

As the fall height increased, there was an increased relationship among BSI_c (r=0.50 to 0.59, p>0.05), and SSI_p (r=0.49 to 0.50, p>0.05) to $F_{2max\text{-}E}$, even after accounting for body mass. Although these variables are weakly correlated, the presence of this relationship may be explained by the stronger relationship between BSIc and SSI_p to MCSA (i.e., r_{BSI} = 0.84 and r_{SSI} = 0.91, p<0.01), relative to body mass (i.e., r_{BSI} = 0.73 and r_{SSI} = 0.80, p<0.05). Bone largely adapts to voluntary loads originating from muscles, and only to a small degree from the force of gravity (i.e., body weight) (Akagi et al., 2008; Frank et al., 2010; H. M. Frost, 1997; Hasegawa et al., 2001; Klein et al., 2002; Kohrt, Barry, & Schwartz, 2009; Nikander et al., 2006). For instance, Nikander and colleagues (2006) compared radius and tibia geometry, and bone and muscle strength estimates across different athletes and controls. They reported that swimming athletes, a sport involving minimal exposure to gravitational forces while in the water, had equally beneficial radius strength as volleyball players and those who participated in high impact racquet sports (Nikander et al., 2006). This high bone strength seen in swimmers was attributed to the vigorous muscle activity involved with competitive swimming (Nikander et al., 2006). Another possible explanation for BSI_c and SSI_p to have increased relationship with $F_{2max\text{-}E}$ may be related to the load-displacement (i.e., the stress-strain curve) curve. Turner (2006) explained that with an increase in force there is a linear displacement of the bone, until the bone yielding point, and the slope of the line represents bone stiffness (Turner, 2006). Therefore, as the force applied to the bone increases, the deformation of the bone also increases, until the fracture point of the bone is reached (Turner, 2006). However, this statement cannot be tested *in vivo* because of the participant safety precautions to prevent falling from heights estimated to cause fracture.

Consistent with my results (r_{mass}=0.79-0.88, p<0.01), body mass has previously been reported to be a strong predictor of $F_{2max\text{-}E}$, especially at fall heights less than 5 cm (Chiu & Robinovitch, 1998; Chou et al., 2001). However, my results indicated that MCSA was also highly correlated with $F_{2max\text{-}E}$ (r_{MCSA}=0.84-0.87, p<0.01), and while the strength of this

relationship decreases after accounting for body mass, it was still somewhat apparent (r_{MCSA}=0.20-0.40, p>0.05). After accounting for body mass, the relationship between F_{2max-E} and MCSA became non-significant, indicating that the high relationship between MCSA and F_{2max-E} is related to the strong relationship between MCSA and body mass (r=0.91, p<0.001). Based on the trends in Figure 11b, I expect a larger sample size would be able to provide evidence for a stronger relationships between F_{1max-E} and both BSI_c and SSI_p; however, I do not expect a larger sample size to strengthen the relationship between MCSA and F_{2max-E}.

6.2 Strength and Limitations

Study Strengths

This is the first time that there is *in vivo* experimental evidence available to support the accuracy of the two-mass, spring-damper model for the prediction of forces on the hand of the outstretched forearm at fall heights up to 25 cm. The experimental evidence supported the accuracy of the model predicted forces that was previously limited to low fall heights of 1, 3, and 5 cm (Chiu & Robinovitch, 1998). Another strength lies in the similarities between the participants involved in the Chiu and Robinovitch (1998) study and those involved in my study. Chiu and Robinovitch (1998) recruited 8 males and 8 females between the ages of 20 and 35 year (mean (±SD): 26±4.6), with a mean body mass of 67±10 kg. These participants are very similar to the participants recruited in this study. For instance, I recruited 5 males and 5 females between the ages of 22 and 30 (mean (±SD): 26±4), with a mean body mass of 74±14.3 kg. This is important because the recruitment of participants that were similar to those participants in Chiu and Robinovitch (1998), provided rationalization for the use of the stiffness and damping variables reported from their study (i.e., generic stiffness and damping variables) in the current study.

The use of human participants allows for: measures of muscle and bone to be obtained *in vivo*, and allows for the acquisition of elbow flexion angles over an array of fall heights during forward facing falls. As previously discussed, the angle of the elbow can drastically alter the magnitude of the force. In order to increase the internal validity of this study, I tried to control for the elbow angle prior to every fall trial by reminding the participant to maintain a straightened arm. However, without casting or splinting the elbow into a straightened position, maintaining a perfectly outstretched arm is impossible due to the

inherent protective characteristic associated with falling from higher heights. Another strength associated with this study was the careful consideration to participant body position prior to the fall. Prior to every fall, I would make certain that the body line was straight from the knees to the shoulders by making the participants extend their hips into the harness. This would ensure the pivot point would be at the knee and not the hip, thereby controlling for lower body positioning. Further, I reminded the participants to keep their dominant arm and hands outstretched during the fall so as to ensure we collected the best possible force data (Appendix C).

This is the first time that estimations of fall related forces have been considered with relation to bone and muscle strength estimates as a function of fall height. The use of bone and muscle strength estimates is important because it broadens the understanding of the factors determining the forces of a person falling forward onto their outstretched forearm. Previous research has established that fall height and body mass were the major factors associated with $F_{1max\text{-}E}$ and $F_{2max\text{-}E}$, respectively (Chiu & Robinovitch, 1998). However, my results have suggested that muscle and bone properties may have relationship with $F_{1max\text{-}E}$ and $F_{2max\text{-}E}$ that may supersede body mass and stature, especially at higher fall heights. However, sample size was low and I expect that a larger sample size would be able to provide the data to support this speculation. Despite the low participant number, the use of bone and muscle properties corroborates the behavior of the experimental results and may perhaps lead to improved force prediction and fracture risk prediction models in the future.

Study Limitations

My study has several limitations. First, I did use generic stiffness and damping elements that were reported in Chiu and Robinovitch (1998), instead of acquiring participant specific stiffness and damping values. However, the use of these generic model parameters have been widely used in the literature and across a variety of ages from children to older adults (Davidson, Chalmers, & Stephenson, 2006a; Davidson et al., 2005; Macdonald et al., 2010; Melton III et al., 2007). Regardless, the use of generic stiffness and damping elements may have lead to discrepancy between $F_{2max\text{-}E}$ and $F_{2max\text{-}M}$ at all fall heights. However, there was no difference in $F_{1max\text{-}E}$ and $F_{1max\text{-}M}$. Therefore comparison of this study to one with participant specific stiffness and damping elements, with similar age, sex, and

anthropometric characteristics, is required in order to determine the impact of participant specific spring and damping elements.

A second limitation to this study lies in the inputting of percentage body segmentation into the model. For instance, the mass of the torso was previously reported to be 49% of the body weight and the mass of the arm was reported to be 5% of the body weight (Clauser et al., 1969). However, Clauser et al (1969) recruited male participants and therefore this percentage based body segmentation may not be generalizable to the female population. Future research should look to acquire participant specific body segmentation through the implementation of DXA scanning. This may allow the model to more closely represent the experimental F_{1max} and F_{2max}.

Another limitation lies in the variability in the force data at fall heights less than 5 cm. One possible explanation for the variability in the fall data may be that the participant's did not carefully focus on maintaining outstretched forearms. This may have lead to fluctuating elbow angles between release and prior to impact, followed by cognitive consideration to straighten the arms. The fluctuation in the elbow angles between release to impact may further lead to the argument that the participants did not have enough time to extend their arms, for fall heights less than 5 cm. However, this is unlikely because simple stimulus response times tested in laboratory situations require 150 ms, while simple stimulus response times outside of the laboratory have been reported at 200 ms (Campbell, Artigas, & Felipe, 1988; Mcleod, 1987; Thorpe, Fize, & Marlot, 1996). The minimum time from trigger (stimulus) to impact for fall heights less than 5 cm ranged from 1082.6 ± 14.1 ms to 1099.4 ± 17.5 ms, these reaction times are significantly greater than the required 150-200 ms (Appendix I). Therefore, all participants had enough time to cognitively program and execute the correct response of maintaining an outstretched arm upon impact at these low fall heights. A further possible explanation could be related to the stiffness and damping coefficients, however, optimization of the model would be required to further elucidate this assumption. The large variability in force data prior to 5 cm , however, may be a strength in disguise. For instance, Chiu and Robinovitch (1998) reported data from three low fall heights: 1, 3, and 5 cm. With this in mind, they may have experienced the same variability and therefore the

testing of their model to experimental data may be the reason for their modification of the stiffness and damping parameters in their participants.

A third limitation to this study lies in the lack of electromyography (EMG) data. EMG should be used to further define the muscle action during a fall, as well as at impact, as previous research indicates that muscle activation affects damping (Milner & Cloutier, 1998). Fourth, while using human participants is highly beneficial for understanding the forces on the outstretched hand, the use of human participants also impedes the use of higher fall heights because of the need for safety precautions. Another limitation to this study is that I assessed data from a small sample of pooled males and females without controlling for sex. Sex has been previously reported to influence radius bone and muscle strength estimates (Mueller et al., 2009; Sumnik et al., 2006), and may influence the forces (Appendix J). However, Chiu and Robinovitch (1998) did indicate that after accounting for body mass, gender had no effect on peak forces, as well as stiffness and damping properties. Finally, while BSI_c and MCSA have been validated at the distal tibia, they have not yet been validated at the distal radius.

6.3 Future Directions

Chiu and Robinovitch (1998) used participant specific stiffness and damping parameters in their model, while I used generic model parameters that were reported in their study. However, this study revealed that using generic model parameters produces similar results between $F_{1max\text{-}E}$ and $F_{1max\text{-}M}$. Regardless, $F_{1max\text{-}E}$ and $F_{1max\text{-}M}$ may become more comparable (i.e., the lines in 9a being very close to on top of one another) if participant specific stiffness and damping elements were used in the model instead of generic parameters. This may result in better fracture risk prediction estimates from the fracture risk equation (Figure 1). Therefore, further research is needed to develop new ways of collecting or estimating the stiffness and damping elements for the model, especially in populations where the collection of experimental data is unsafe.

Although the relationship between bone and muscle strength estimates and force peaks appeared to increase with height, there appeared to be a decreased relationship around 20 cm. While this was not a significant reduction in the relationship, it warrants some discussion and mention of possible future study direction. One possible explanation for the

decreased relationship between the forces and MCSA around 20 cm may correspond to an increase in elbow flexion. More specifically, however, the decreased relationship may pertain to those individuals with larger MCSA having an increased capacity to comply with maintaining an extended arm at impact, especially at higher fall heights when the force is high. My results indicate that the female participants, with lower MCSA than the males, had higher elbow flexion angles relative to the male participants at all fall heights (Appendix H). The higher degree of elbow flexion in the females was most prominent after 5 cm (Appendix H). The results suggest that the female participants may not have had the muscle size and strength to maintain outstretched arms at impact for heights greater than 5 cm. However, further research should look at recruiting a larger sample of males and females to confirm this speculation.

As previously mentioned, fracture risk prediction requires the understanding of both the applied load and bone strength. This study focused on the force applied to the hand of the outstretched forearm during a fall, with a pilot investigation into the influence of estimated bone and muscle strength parameters. Future research should look to validating the fracture risk equation presented in Figure 1. More specifically, the information acquired using the two-mass, spring-damper model could be entered as the numerator of the fracture risk prediction equation. Further, bone and muscle strength estimates may be acquired using high resolution pQCT imaging, combined with the computer simulated modeling of the bone strength using finite element analyses. These bone and muscle parameters may then be entered into the denominator of the fracture risk equation (Figure 1). This analysis may yield a more reliable estimate of an individual's fracture risk as opposed to bone densitometry or bone strength modeling from high resolution CT images (i.e., finite element analysis) alone.

6.4 Summary and Conclusion

Overall, I have shown that the mathematical model, defined by Chiu and Robinovitch (1998), does predict $F_{1max\text{-}E}$, when using generic stiffness and damping variables, but not $F_{2max\text{-}E}$. While previous research experimented to a fall height of 5 cm, it is difficult to accurately determine the relationship between force and fall height from a 3 data points at short fall heights. Therefore, I have reported experimental force results at heights up to 25 cm. I also revealed a moderate and positive correlation of BSI_c, SSI_p, MCSA, body mass, and stature to

$F_{1max\text{-}E}$ and $F_{2max\text{-}E}$, and these relationships appeared to get stronger with increasing fall height. Further, I report that MCSA was more highly correlated to $F_{1max\text{-}E}$ than the other anthropometric variables, both before and after accounting for body mass. Similarly, BSI_c and SSI_p were more strongly related to $F_{2max\text{-}E}$. While these relationships decreased after accounting for body mass, they are still evident. I expect that a larger sample size would be able to provide stronger relationships between F_{1max} and bone and muscle strength estimates. The next step is to optimize the model and reassess the results to determine how the stiffness and damping elements affect the model. A larger sample size is needed to confirm whether incorporating bone and muscle strength estimates into fall force prediction models could enhance forearm fracture risk assessments.

7.0 REFERENCES

Adams, J. E. (2009). Quantitative computed tomography. *European Journal of Radiology, 71*(3), 415-424.

Akagi, R., Takai, Y., Kato, E., Fukuda, M., Wakahara, T., Ohta, M., et al. (2008). Relationships between muscle strength and indices of muscle cross sectional area determined during maximal voluntary contraction in middle aged and elderly individuals. *Journal of Strength and Conditioning Research, 23*(4), 1258-1262.

Ammann, P., & Rizzoli, R. (2003). Bone strength and its determinants. *Osteoporosis International, 14*(Suppl 3), S13-S18.

Augat, P., Gordon, C. L., Lang, T. F., Iida, H., & Genant, H. K. (1998). Accuracy of cortical and trabecular bone measurements with peripheral quantitative computed tomography (pQCT). *Physics in Medicine and Biology, 43*, 2873-2884.

Augat, P., Iida, H., Jiang, Y., Diao, E., & Genant, H. K. (1998). Distal radius fractures: Mechanisms of injury and strength prediction by bone mineral assessment. *Journal of Orthopaedic Research, 16*(5), 629-635.

Augat, P., Reeb, H., & Claes, L. E. (1996). Prediction of fracture load at different skeletal sites by geometric properties of the cortical shell. *Journal of Bone and Mineral Research, 11*(9), 1356-1363.

Barrett-Connor, E., Sajjan, S. G., Siris, E. S., Miller, P. D., Chen, Y. T., & Markson, L. E. (2008). Wrist fracture as a predictor of future fractures in younger versus older postmenopausal women: Results from the national osteoporosis risk assessment (NORA). *Osteoporosis International, 19*(5), 607-613.

Bolotin, H. H. (1998). Analytic and quantitative exposition of patient-specific systematic inaccuracies inherent in planar DXA-derived in vivo BMD measurements. *Medical Physics, 25*(2), 139-151.

Bolotin, H. H. (2007). DXA in vivo BMD methodology: An erroneous and misleading research and clinical gauge of bone mineral status, bone fragility, and bone remodelling. *Bone, 41*(1), 138-154.

Bonjour, J. P., Chevalley, T., Ferrari, S., & Rizzoli, R. (2009). The importance and relevance of peak bone mass in the prevalence of osteoporosis. *Salud Pública De México, 51*(Suppl. 1), S5-S17.

Bouxsein, M. L., & Seeman, E. (2009). Quantifying the material and structural determinants of bone strength. *Best Practice and Research. Clinical Rheumatology, 23*(6), 741-753.

Burge, R., Dawson-Hughes, B., Solomon, D. H., Wong, J. B., King, A., & Tosteson, A. (2007). Incidence and economic burden of osteoporosis related fractures in the united states, 2005 - 2025. *Journal of Bone and Mineral Research, 22*(3), 465-475.

Campbell, F. W., Artigas, J. M., & Felipe, A. (1988). Visual reaction time versus action time. *Ophthalmic and Physiological Optics, 8*(1), 60-62.

Chalmers, D. J., Marshall, S. W., Langley, J. D., Evans, M. J., Brunton, C. R., Kelly, A. M., et al. (1996). Height and surfacing as risk factors for injury in falls from playground equipment: A case control study. *Injury Prevention, 2*(2), 98-104.

Chiu, J., & Robinovitch, S. N. (1998). Prediction of upper extremity impact forces during falls on the outstretched hand. *Journal of Biomechanics, 31*(12), 1169-1176.

Chou, P. H., Chou, Y. L., Lin, C. J., Su, F. C., Lou, S. Z., Lin, C. F., et al. (2001). Effect of elbow flexion on upper extremity impact forces during a fall. *Clinical Biomechanics, 16*(10), 888-894.

Chou, P. H., Lou, S. Z., Chen, H. C., Chiu, C. F., & Chou, Y. L. (2009). Effect of various forearm axially rotated postures on elbow load and elbow flexion angle in one armed arrest of a forward fall. *Clinical Biomechanics, 24*(8), 632-636.

Chung, K. C., & Spilson, S. V. (2001). The frequency and epidemiology of hand and forearm fractures in the united states. *Journal of Hand Surgery, 26*(5), 908-915.

Clauser, C. E., McConville, J. T., & Young, J. W. (1969). *Weight, volume, and center of mass of segments of the human body* No. AD0710622). Wright Patterson Airforces Base, Dayton, OH: National Technical Information Service.

Cummings, S. R., & Nevitt, M. C. (1994). Non-skeletal determinants of fractures: The potential importance of the mechanics of falls. *Osteoporosis International, S1*, S67-S70.

Davidson, P. L., Chalmers, D. J., & Stephenson, S. C. (2006). Prediction of distal radius fracture in children, using a biomechanical impact model and case-control data on playground free falls. *Journal of Biomechanics, 39*(3), 503-509.

Davidson, P. L., Chalmers, D. J., & Wilson, B. D. (2004). Stochastic-rheological simulation of free-fall arm impact in children: Application to playground injuries. *Computer Methods in Biomechanics and Biomedical Engineering, 7*(2), 63-71.

Davidson, P. L., Goulding, A., & Chalmers, D. J. (2003). Biomechanical analysis of arm fracture in obese boys. *Journal of Paediatrics and Child Health, 39*(9), 657-664.

Davidson, P. L., Mahar, B., Chalmers, D. J., & Wilson, B. D. (2005). Impact modeling of gymnastic back-handsprings and dive-rolls in children. *Journal of Applied Biomechanics, 21*(2), 115-128.

DeGoede, K. M., & Ashton-Miller, J. A. (2002). Fall arrest strategy affects peak hand impact force in a forward fall. *Journal of Biomechanics, 35*(6), 843-848.

Engelke, K., Libanati, C., Liu, Y., Wang, H., Austin, M., Fuerst, T., et al. (2009). Quantitative computed tomography (QCT) of the forearm using general purpose spiral whole body CT scanners: Accuracy, precision, and comparison with dual-energy x-ray absorptiometry (DXA). *Bone, 45*(1), 110-118.

Ferrari, S. L., Chevalley, T., Bonjour, J. P., & Rizzoli, R. (2006). Childhood fractures are associated with decreased bone mass gain during puberty: An early marker of persistent bone fragility? *Journal of Bone and Mineral Research, 21*(4), 501-507.

Ferretti, J., Capozza, R. F., Cointry, G. R., Garcia, S. L., Plotkin, H., Alvarez Filguiera, M. L., et al. (1998). Gender related differences in the relationship between densitometric values of whole body bone mineral content and lean body mass in humans between 2 and 87 years of age. *Bone, 22*(6), 683-690.

Ferretti, J. L., Capozza, R. F., & Zanchetta, J. R. (1996). Mechanical validation of a tomographic (pQCT) index for non-invasive estimation of rat femur bending strength. *Bone, 18*(2), 97-102.

Fiissel, D., Pattison, G., & Howard, A. (2005). Severity of playground fractures - play equipment versus standing height falls. *Injury Prevention, 11*(6), 337-339.

Frank, A. W., Lorbergs, A. L., Chilibeck, P. D., Farthing, J. P., & Kontulainen, S. A. (2010). Muscle cross sectional area and grip torque contraction types are similarly related to pQCT derived bone strength indices in the radii of older healthy adults. *Journal of Musculoskeletal and Neuronal Interactions, 10*(2), 136-141.

Frost, H. M. (1997). On our age related bone loss: Insights from a new paradigm. *Journal of Bone and Mineral Research, 12*(10), 1539-1546.

Frost, H. M. (1987). Bone "mass" and the "mechanostat": A proposal. *The Anatomical Record, 219*(1), 1-9.

Frykman, G. (1967). Fracture of the distal radius including sequelae - shoulder-hand-finger syndrome, disturbance in the distal radio-ulnar joint and impairment of nerve function. A clinical and experimental study. *Acta Orthopaedica Scandinavica,* (S108), S111.

Fukunaga, T., Miyatani, M., Tachi, M., Kouzaki, M., Kawakami, Y., & Kanehisa, H. (2001). Muscle volume is a major determinnat of joint torque in humans. *Acta Physiologica Scandinavica, 172*(4), 249-255.

Griffith, J. F., Engelke, K., & Genant, H. K. (2010). Looking beyond bone mineral density: Imaging assessment of bone quality. *Annals of the New York Academy of Sciences, 1192*(1), 45-56.

Grood, E. S., & Suntay, W. J. (1983). A joint coordinate system for the clinical description of three dimensional motions: Application to the knee. *Journal of Biomechanical Engineering, 105*, 136-143.

Haapasalo, H., Kontulainen, S., Sievanen, H., Kannus, P., Jarvinen, M., & Vuori, I. (2000). Exercise-induced bone gain is due to enlargement in bone size without a change in volumetric bone density: A peripheral quantitative computed tomography study of the upper arms of male tennis players. *Bone, 27*(3), 351-357.

Hasegawa, Y., Schneider, P., & Reiners, C. (2001). Age, sex, and grip strength determin architectural bone parameters assessed by peripheral quantitative computed tomography (pQCT) at the human radius. *Journal of Biomechanics, 34*(4), 497-503.

Hayes, W., & Bouxsein, M. L. (1997). Biomechanics of cortical and trabecular bone: Implications for assessment of fracture risk. *Basic orthopaedic biomechanics*. Philadelphia: Lippincott - Raven Publishers.

Hayes, W. C., Piazza, S. J., & Zysset, P. K. (1991). Biomechanics of fracture risk prediction of the hip and spine by quantitative computed tomography. *Radiologic Clinics of North America, 29*(1), 1-18.

Howard, A. W., Macarthur, C., Rothman, L., Willan, A., & Macpherson, A. K. (2009). School playground surfacing and arm fractures in children: A cluster randomized trial comparing sand to wood chip surfaces. *PLoS Medicine, 6*(12), e1000195-e1000204.

Johnell, O., & Kanis, J. (2006). Epidemiology of osteoporotic fractures. *Osteoporosis International, 16*(2), S3-S7.

Kawalilak, C. E., Baxter-Jones, A. D. G., Faulkner, R. A., Bailey, D. A., & Kontulainen, S. A. (2010). Does childhood and adolescence fracture influence bone mineral content in young adulthood? *Applied Physiology, Metabolism, and Nutrition, 35*, 1-9.

Keaveny, T. M., & Bouxsein, M. L. (2008). Perspective: Theoretical implications of the biomechanical fracture threshold. *Journal of Bone and Mineral Research, 23*(10), 1541-1547.

Khosla, S., Melton III, J., Dekutoski, M. B., Achenbach, S. J., Oberg, A. L., & Riggs, B. L. (2003). Incidence of childhood distal forearm fractures over 30 years: A population based study. *Journal of the American Medical Association, 290*, 1479-1485.

Klein, C. S., Allman, B. L., Marsh, G. D., & Rice, C. L. (2002). Muscle size, strength, and bone geometry in the upper limbs of young and old men. *The Journals of Gerontology, Series A: Biological Sciences and Medical Sciences, 57*(7), M455-M459.

Klotzbuecher, C. M., Ross, P. D., Landsman, P. B., Abbott, T. A., 3rd, & Berger, M. (2000). Patients with prior fractures have an increased risk of future fractures: A summary of the literature and statistical synthesis. *Journal of Bone and Mineral Research, 15*(4), 721-739.

Kohrt, W., Barry, D. W., & Schwartz, R. S. (2009). Muscle forces or gravity: What predominates mechanical loading on bone? *Medicine and Science in Sports and Exercise, 41*(11), 2050-2055.

Kontulainen, S. A., Hughes, J. M., Macdonald, H. M., & Johnston, J. D. (2007). The biomechanical basis of bone strength development during growth. *Medicine and Sport Science, 51*, 13-32.

Kontulainen, S. A., Johnston, J. D., Liu, D., Leung, C., Oxland, T. R., & McKay, H. A. (2008). Strength indices from pQCT imaging predict up to 85% of variance in bone failure properties at tibial epiphysis and diaphysis. *Journal of Muscusloskeletal Neuronal Interactions, 8*(4), 401-409.

Laforest, S., Robitaille, Y., Lesage, D., & Dorval, D. (2001). Surface characteristics, equipment height, and the occurrence and severity of playground injuries. *Injury Prevention, 7*(1), 35-40.

Laing, A. C., & Robinovitch, S. N. (2009). Low stiffness floors can attenuate fall related femoral impact forces by up to 50% without substantially impairing balance in older women. *Accident: Analysis and Prevention, 41*(3), 642-650.

Laing, A. C., Tootoonchi, I., Hume, P. A., & Robinovitch, S. N. (2006). Effect of compliant flooring on impact force during falls on the hip. *Journal of Orthopaedic Research, 24*(7), 1405-1411.

Landin, L. A. (2010). Fracture epidemiology. In M. Benson, J. Fixsen, M. Macnicol & K. Parsch (Eds.), *Children's orthopaedics and fractures* (3rd Edition ed., pp. 665-669). London: Springer - Verlag London Ltd.

Lo, J., & Ashton-Miller, J. A. (2008). Effect of upper and lower extremity control strategies on predicted injury risk during simulated forward falls: A study in healthy young adults. *Journal of Biomechanical Engineering, 130*(4), 041015-1-041015-8.

Lo, J., McCabe, G. N., DeGoede, K. M., Okuizumi, H., & Ashton-Miller, J. A. (2003). On reducing hand impact force in forward falls: Results of a brief intervention in young males. *Clinical Biomechanics, 18*(8), 730-736.

Lochmuller, E. M., Lill, C. A., Kuhn, V., Schneider, E., & Eckstein, F. (2002). Radius bone strength in bending, compression, and falling and its correlation with clinical densitometry at multiple sites. *Journal of Bone and Mineral Research, 17*(9), 1629-1638.

Loder, R. T. (2008). The demographics of playground equipment injuries in children. *Journal of Pediatric Surgery, 43*(4), 691-699.

Macdonald, H. M., Nishiyama, K. K., Kang, J., Hanley, D. A., & Boyd, S. K. (2010). Age related patterns of trabecular and cortical bone loss differ between sexes and skeletal

sites: A populations based HR-pQCT study. *Journal of Bone and Mineral Research, Epub ahead of print*

MacNeil, J.A., Boyd, S.K. (2008). Bone strength at the distal radius can be estimated from high-resolution peripheral quantitative computed tomography and the finite element model. *Bone, 42*(6), 1203-1213.

Martin, R. B., Burr, D. B., & Sharkey, N. A. (1998). *Skeletal tissue mechanics*. New York, New York: Springer.

Maynard, L. M., Guo, S. S., Chumlea, W. C., Roche, A. F., Wisemandle, W. A., Zeller, C. M., et al. (1998). Total body and regional bone mineral content and areal bone mineral density in children aged 8-18 years: The Fels Longitudinal Study. *American Journal of Clinical Nutrition, 68*(5), 1111-1117.

Mcleod, P. (1987). Visual reaction time and high speed ball games. *Perception, 16*(1), 49-59.

Melone, C. P. (1984). Articular fractures of the distal radius. *Orthopaedic Clinics of North America, 15*, 217-236.

Melton III, J. L., Riggs, B. L., van Lenthe, G. H., Achenbach, S. J., Muller, R., Bouxsein, M. L., et al. (2007). Contribution of in vivo structural measurements and load/strength ratios to the determination of forearm fracture risk in postmenopausal women. *Journal of Bone and Mineral Research, 22*(9), 1442-1448.

Melton, L. J., Chao, E. Y. S., & Lane, J. (1988). Biomechanical aspects of fractures. In B. L. Riggs, & L. J. Melton (Eds.), *Osteoporosis: Etiology, diagnosis, and management* (pp. 111-131). New York: Raven Press.

Milner, T. E. (2002). Adaptation to destabilizing dynamics by means of muscle cocontraction. *Experimental Brain Research, 143*(4), 406-416.

Milner, T. E., & Cloutier, C. (1998). Damping of the wrist joint during voluntary movement. *Experimental Brain Research, 122*, 309-317.

Mueller, T. L., van Lenthe, G. H., Stauber, M., Gratzke, C., Exkstein, F., & Muller, R. (2009). Regional, age and gender differences in architectural measures of bone quality and their correlation to bone mechanical competence in the human radius of an elderly population. *Bone, 45*, 882-891.

Muller, M. E., Webber, C. E., & Bouxsein, M. L. (2003). Predicting the failure load of the distal radius. *Osteoporosis International, 14*(4), 345-352.

Myers, E. R., Hecker, A. T., Rooks, D. S., Hipp, J. A., & Hayes, W. C. (1993). Geometric variables from DXA of the radius predict forearm fracture load in vitro. *Calcified Tissue International, 52*, 199-204.

Myers, E. R., Sebeny, E. A., Hecker, A. T., Corcoran, T. A., Hipp, J. A., Greenspan, S. L., et al. (1991). Correlations between photon absorption properties and failure load of the distal radius in vitro. *Calcified Tissue International, 49*, 292-297.

National Council on Radiation Protection and Measurements (NCRP). (2009). *Ionizing radiation exposure of the population of the united states* No. 160)

Nielson, S. P. (2000). The fallacy of BMD: A critical review of the diagnostic use of dual x-ray absorptiometry. *Clinical Rheumatology, 19*(3), 174-183.

Nikander, R., Sievanen, H., Heinonen, A., Daly, R. M., Uusi-Rasi, K., & Kannus, P. (2010). Targeted exercise against osteoporosis: A systematic review and meta-analysis for optimising bone strength throughout life. *BMC Medicine, 8*, 47-63.

Nikander, R., Sievanen, H., Uusi-Rasi, K., Heinonen, A., & Kannus, P. (2006). Loading modalities and bone structures at nonweight bearing upper extremity and weight bearing lower extremity: A pQCT study of adult female athletes. *Bone, 39*(4), 886-894.

Njeh, C. F., Fuerst, T., Hans, D., Blake, G. M., & Genant, H. K. (1999). Radiation exposure in bone mineral density assessment. *Applied Radiation and Isotopes, 50*(1), 215-236.

Norton, K., Carter, L., Olds, T., & Marfell-Jones, M. (2001). *International standards for anthropometric assessment*. Underdale, Australia: The International Society for the Advancement of Kinanthropometry.

Petit, M. A., Beck, T. J., & Kontulainen, S. A. (2005). Examining the developing bone: What do we measure and how do we do it? *Journal of Musculoskeletal & Neuronal Interactions, 5*(3), 213-224.

Rauch, F., Bailey, D. A., Baxter-Jones, A. D. G., Mirwald, R. L., & Faulkner, R. A. (2004). The 'muscle-bone unit' during the pubertal growth spurt. *Bone, 34*(5), 771-775.

Rauch, F., & Schoenau, E. (2001). Changes in bone density during childhood and adolescence: An approach based on bone's biological organization. *Journal of Bone and Mineral Research, 16*(4), 597-604.

Rennie, L., Court-Brown, C. M., Mok, J. Y. Q., & Beattie, T. F. (2007). The epidemiology of fractures in children. *Injury, 38*(8), 913-922.

Riggs, B. L., & Melton, L. J. I. (1995). The worldwide problem of osteoporosis: Insights afforded by epidemiology. *Bone, 17*(Suppl 5), 505-511.

Riggs, B. L., Melton Iii, L. J.,3rd, Robb, R. A., Camp, J. J., Atkinson, E. J., Peterson, J. M., et al. (2004). Population-based study of age and sex differences in bone volumetric density, size, geometry, and structure at different skeletal sites. *Journal of Bone and Mineral Research, 19*(12), 1945-1954.

Robinovitch, S. N., & Chiu, J. (1998). Surface stiffness affects impact force during a fall on the outstretched hand. *Journal of Orthopaedic Research, 16*(3), 309-313.

Schoenau, E., Neu, C. M., Rauch, F., & Manz, F. (2001). The development of bone strength at the proximal radius during childhood and adolescence. *Journal of Clinical Endocrinology & Metabolism, 86*(2), 613-618.

Schousboe, J. T., Fink, H. A., Taylor, B. C., Stone, K. L., Hillier, T. A., Nevitt, M. C., et al. (2005). Association between self-reported prior wrist fractures and risk of subsequent hip and radiographic vertebral fractures in older women: A prospective study. *Journal of Bone and Mineral Research, 20*(1), 100-106.

Seeman, E. (2001). Clinical review 137: Sexual dimorphism in skeletal size, density, and strength. *Journal of Clinical Endocrinology and Metabolism, 86*(10), 4576-4584.

Seeman, E. (2008). Bone quality: The material and structural basis of bone strength. *Journal of Bone and Mineral Metabolism, 26*(1), 1-8.

Seeman, E., & Delmas, P. D. (2006). Bone quality: The material and structural basis of bone strength and fragility. *New England Journal of Medicine, 354*(21), 2250-2261.

Seibel, M. J. (2007). Bone turnover in nutrition related disorders. *Wiener Medizinische Wochenschrift, 157*(23), 582-588.

Serway, R. A., & Jewett Jr., J. W. (Eds.). (2004). *Physics for scientists and engineers with modern physics* (6th Edition). Toronto, Ontario: Brooks/Cole - Thompsom Learning.

Sherker, S., & Ozanne-Smith, J. (2004). Are current playground safety standards adequate for preventing arm fractures? *The Medical Journal of Australia, 180*(11), 562-565.

Sievanen, H., Koskue, V., Rauhio, A., Kannus, P., Heinonen, A., & Vuori, I. (1998). Peripheral quantitative computed tomography in human long bones: Evaluation of in vitro and in vivo precision. *Journal of Bone and Mineral Research, 13*(5), 871-882.

Spadaro, J. A., Werner, F. W., Brenner, R. A., Fortino, M. D., Fay, L. A., & Edwards, W. T. (1994). Cortical and trabecular bone contribute strength to the osteopenic distal radius. *Journal of Orthopaedic Research, 12*(2), 211-218.

Sran, M. M., & Robinovitch, S. N. (2008). Preventing fall related vertebral fractures: Effect of floor stiffness on peak impact forces during backward falls. *Spine, 33*(17), 1856-1862.

Steele, J., & Mays, S. (1995). Handedness and directional asymmetry in the long bones of the human upper limb. *International Journal of Osteoarchaeology, 5*(1), 39-49.

Stratec Medisintechnik GmbH. (2004). XCT 2000 manual software version 5.50.

Sumnik, Z., Land, C., Coburger, S., Neu, C., Manz, F., Hrach, K., et al. (2006). The muscle-bone unit in adulthood: Influence of sex, height, age and gynecological history on the bone mineral content and muscle cross sectional area. *Journal of Musculoskeletal Neuronal Interactions, 6*(2), 195-200.

Tan, J. S., Eng, J. J., Robinovitch, S. N., & Warnick, B. (2006). Wrist impact velocities are smaller in forward falls than backward falls from standing. *Journal of Biomechanics, 39*(10), 1804-1811.

Thorpe, S., Fize, D., & Marlot, C. (1996). Speed of processing in the human visual system. *Nature, 381*, 520-522.

Turner, C. H. (2006). Bone strength: Current concepts. *New York Academy of Sciences,* , 429-446.

Ural, A. (2009). Prediction of Colles' fracture load in human radius using cohesive finite element modeling, *Journal of Biomechanics, 42*, 22-28.

Vatanparast, H., Baxter-Jones, A. D. G., Faulkner, R. A., Bailey, D. A., & Whiting, S. J. (2005). Positive effects of vegetable and fruit consumption and calcium intake on bone mineral accrual in boys during growth from childhood to adolescence: The university of saskatchewan pediatric bone mineral accrual study. *American Journal of Clinical Nutrition, 82*(3), 700-706.

Vincent, W. (2005). *Statistics in Kinesiology* (3rd edition). Champaign, Illinois. Human Kinetics.

Wang, X., & Puram, S. (2004). The toughness of cortical bone and its relationship with age. *Annals of Biomedical Engineering, 32*(1), 123-135.

Wu, G., van der Helm, F. C., Veeger, H. E., Makhsous, M., Van Roy, P., Anglin, C., et al. (2005). ISB recommendations on definitions of joint coordinate systems of various joints for the reporting of human joint motion - part II: Shoulder, elbow, wrist and hand. *Journal of Biomechanics, 38*(5), 981-992.

Zhang, L. Q., & Rymer, W. Z. (1997). Simultaneous and nonlinear identification of mechanical and reflex properties of human elbow joint muscles. *IEEE Transactions on Biomedical Engineering, 44*(12), 1192-1209.

Zhang, P., Hamamura, K., & Yokota, H. (2008). A brief review of bone adaptation to unloading. *Genomics, Proteomics, and Bioinformatics, 6*(1), 4-7.

8.0 APPENDICES

APPENDIX A: DEMOGRAPHIC INFORMATION QUESTIONNAIRE

DATE: _____ NAME: _____

SUBJECT ID: _____ DOB: _____

LIMB DOMINANCY AND MUSCULOSKELETAL HEALTH QUESTIONNAIRE

Please answer the following questions to the best of your ability. You do not need to answer any question you do not feel comfortable answering. These questions are asked for inclusion/exclusion criteria only.

1. **Which hand do you use the most when: writing, catching and throwing a ball, cutting with scissors, etc (i.e., which had is your dominant hand)?**
   a. Left
   b. Right
   c. I am mixed-handed
   d. I don't know

2. **Have you ever had a broken "wrist"?**
   a. Yes
   b. No
   c. Not Sure

If yes, please indicate: ☐ Left Date(s): _____

☐ Right Date(s): _____

3. **Have you broken any other bone(s)?**
   a. Yes
   b. No
   c. Not Sure

If yes, please indicate:

Bone(s)	Side	Date(if known)

4. **Did you break any bones more than once?**
    a. Yes
    b. No
    c. Not Sure

If yes, please indicate:

Bone(s)	Side	Date (if known)

APPENDIX B: CONSENT FORM

RESEARCH PARTICIPATION INFORMATION AND CONSENT FORM

TITLE: Validation of Fall Force Prediction Models

REB STUDY # : BIO#09-108

PRINCIPAL INVESTIGATORS

Joel Lanovaz
Assistant Professor
Phone: 306.966.1073
College of Kinesiology
87 Campus Drive
Saskatoon, SK
S7N 5B2

Saija Kontulainen
Assistant Professor
Phone: 306.966.1077
College of Kinesiology
87 Campus Drive
Saskatoon, SK
S7N 5B2

James Johnston
Assistant Professor
Phone: 306.966.1468
Department of
Mechanical Engineering
57 Campus Drive
Saskatoon, SK
S7N 5A9

STUDENT RESEARCHERS:

Devin Glennie, Supervisors: Joel Lanovaz, Saija Kontulainen, James Johnston

Chantal Kawalilak, Supervisor: Saija Kontulainen

David Kobylak, Supervisor: Joel Lanovaz

INTRODUCTION: You are invited to take part in this research study because we are interested in understanding the sudden forces applied to the forearm when healthy adults fall onto their outstretched hands.

If you decide not to take part, you do not have to provide a reason and it will not affect your relationship with any of the researchers. If you decide to take part in this study, you are still free to withdraw at any time and without giving any reasons for your decision.

This consent form may contain words that you do not understand. Please ask the principal investigators or the study staff to explain any words or information that you do not clearly understand. You may ask as many questions as you need to understand what the study involves. Please feel free to discuss this with your family, friends or family physician.

PURPOSE: The purpose of this study is to find out why some people fracture their wrists when they fall and why other people do not. Currently, wrist fractures are the second most common lifetime injury and they regularly occur when people fall on their extended arm and cushion the fall using their hands. However, not everyone suffers a fracture when they fall. Figuring out what reasons cause these fractures to occur should help lower the number of these fractures in the future.

The main goal of this study is to use experimental data gathered during fall tests to verify that the fracture risk prediction methods created by other researchers are correct. These methods have been established in similar studies conducted on adults in other institutions. If correct, these methods will be applied in future studies that assess forearm and wrist fracture risk in children and older adults.

STUDY DESIGN: This study involves you falling onto your extended hand. These falls will be performed at a low height with your hand 1-25 centimeters above a foam cushion. Falls will be done in the forward position. A safety harness and tether will be used to adjust you into the proper orientation.

STUDY PROCEDURES: If you choose to participate, you will be asked to perform several forward facing fall tests onto your extended at different heights. In the forward fall test position, you will be asked to kneel on all fours limbs before a harness lifts up your upper body and arms off of the ground. You will start at a height of 0 cm so that the researchers can gather neutral information about your body, and make adjustments to your body's positioning (i.e., making sure your hands are outstretched according to study protocol). Once this data is collected you will be dropped (by releasing the tether attached to the harness) at randomized heights between 1-25 cm, inclusive, and then asked if you felt any pain. If you want to continue the test, you may be raised to a slightly higher height and the test will be repeated. If you feel pain and do not want to continue, the tests will be stopped immediately.

Before the fall tests, you will be asked to fill out a questionnaire regarding your demographic background and bone and muscle health. You may refuse to fill questionnaire if you want. Your height and weight will also be measured and recorded. You will then be fitted with the safety harness and several data measuring devices. These little devices will be taped to your arms and shoulders. It may be necessary to shave off a small patch of hair from your arm to apply them.

Setup prior to the fall tests may take as much as 30 minutes. However, the total time for the fall tests may be as little as a few minutes. The total time required by you should be approximately 1.5 hours.

Following drop testing procedures, you will accompany one of the researchers to PAC 357 so as to obtain bone and muscle scans with using peripheral quantitative computed tomography (pQCT). First, the length of your dominant arm will be measured with a tape measure. Your dominant arm will be scanned using pQCT at two difference sites: one close to the wrist (4% forearm length) and one closer to your elbow (65% forearm length).

Finally, you will accompany one of the researchers to PAC 359 so as to obtain bone scans using high resolution peripheral quantitative computed tomography (HR pQCT/ XtremeCT). HR pQCT will be used to scan the distal forearm (1 mm from the distal endplate). Data obtained from HR pQCT will be used to create a finite element analysis of the radius and allow for better assess bone strength at the distal forearm.

BENEFITS: If you choose to participate in this study, there may not be direct benefits to you. However, you will learn about your individual force on your forearms and you will learn about your bone and muscle health. It is hoped that the information gained from this study can be used in the future to better predict forces associated with falls and enhance muscle and bone strength assessments in other people. We hope that the information gained from this study can be used in the future to reduce the number of wrist fractures of other people.

RISKS AND DISCOMFORTS:

If you choose to participate in this study, the following are possible:

- Irritation or chafing to the skin from the data sensors and safety harness (common)
- Slight pain or stinging when removing the data sensors (very common)
- Discomfort or mild pain in the wrist after performing fall tests (common)
- Wrist fracture during fall tests (very rare)

Further, you will be exposed to small amounts of radiation during the pQCT scan. The total amount of radiation to which your forearm will be exposed is very low, an average of less than 4 µSv (less than 1 µSv, using pQCT and approximately 3 µSv, using HR pQCT). The typical exposure from a routine dental x-ray, for example, ranges between 90-150 µSv.

COST AND REIMBURSEMENTS: There will be no cost to you for participation in this study and the researchers will provide no reimbursements.

RESEARCH-RELATED INJURY: In the case of a medical emergency related to the study, you should seek immediate care and, as soon as possible, notify the study's principal investigator. Necessary medical treatment will be made available at no cost to you. By signing this document, you do not waive any of your legal rights.

CONFIDENTIALITY: While complete subject anonymity cannot be guaranteed, every effort will be made to ensure that the information you provide for this study is kept entirely confidential. Your name will not be attached to any information, nor mentioned in any study report, nor be made available to anyone except the research team. It is the intention of the research team to publish results of this research in scientific journals and to present the findings at related conferences and workshops.

Most research findings will be reported in aggregate form without any reference to specific participants. In the event individual data are used, only participant codes will be referenced and your identity will not be revealed. Some digital still images and video are taken during data collection for reference. These images are kept confidential. If an image is used for publication purposes, it will be altered to remove all information that could be used to identify a specific individual.

Data are stored on password protected digital media (i.e., DVD) in a locked lab/office in the College of Kinesiology to which only the researchers will have access. The data will be used

for dissertation and publication purposes only, and will be retained for a minimum of five years. Normally data is retained for a period of five years post-publication, after which time it may be destroyed.

NEW INFORMATION: The principal investigators will tell you about new information that may affect your health, welfare, or willingness to stay in this study.

VOLUNTARY WITHDRAWAL FROM THE STUDY: If you do decide to take part in this study, you are still free to withdraw at any time and without giving reasons for your decision. There will be no penalty or loss of benefits to which you are otherwise entitled, and your future medical care will not be affected. If you choose to enter the study and then decide to withdraw at a later time, all data collected about you will destroyed.

WITHDRAWAL INITIATED BY THE INVESTIGATOR OR SPONSOR: You may be withdrawn from the study if:

- Staying in the study would be harmful.
- You need treatment not allowed in the study.
- You fail to follow instructions.
- You become pregnant.
- The study is cancelled by the sponsor for administrative or other reasons.

AFTER COMPLETION OF THE STUDY: Once the study is complete, you may request a lay summary of the aggregate results by contacting the investigators.

CONTACT INFORMATION: If you have any questions about this study or your care/treatment or desire further information about this study before or during participation, you can contact either Dr. Joel Lanovaz by phone at 306-966-1073, or by email at joel.lanovaz@usask.ca.

If you have any questions about your rights as a research subject or concerns about the study, you should contact the Chair of the Biomedical Research Ethics Board, c/o the Ethics Office, University of Saskatchewan, at 306-966-4053.

This study has been reviewed and approved on ethical grounds by the University of Saskatchewan Biomedical Research Ethics Board. The Research Ethics Board reviews human research studies. It protects the rights and welfare of the people taking part in those studies.

CONSENT TO PARTICIPATE

I have read (or someone has read to me) the information in this consent form. I understand the purpose and procedures, the possible risks and benefits of the study. I was given sufficient time to think about it. I had the opportunity to ask questions and have received satisfactory answers to all of my questions.

I am free to withdraw from this study at any time for any reason and the decision to stop taking part will not affect my future medical care. I agree to follow the principal investigator's instructions.

I voluntarily consent to take part in this research study and give permission to the use and disclosure of my de-identified personal health information collected for the research purposes described above.

By signing this document I do not waive any of my legal rights. I will be given a signed copy of this consent form.

I authorize the researchers to contact me in the future for research purposes. Such research will have been given ethics approval. Please check one of the following:

- ☐ **Yes**
- ☐ **No**

Printed Name of Participant:	Signature:	Date:
_____	_____	_____
Printed Name of Researcher:	Signature:	Date:
_____	_____	_____

APPENDIX C: DROP TEST BODY POSITION PROTOCOL

Forward Fall Body Position

The following is a description of the body position and fall testing procedure that the participant's were required to comply with during their participation in this study.

- Participants began on their knees, shins, and dorsal foot-ground contact with their hand outstretched.
- The electromagnet was turned on so as to allow contact between the magnet and the metal plate tethered to the harness. The hand crank was used to raise the participant's trunk to the pre-determined heights.
- Right and left hands were staggered so that the ground impact occurred on the right hand prior to the left. The right hand was directly over the force plate.
- The electromagnet, suspending the participant's trunk above the force plate, was released at random time intervals.
- Prior to release, I checked the body line so that a straight line could be drawn from the knees to the shoulders of the participants. Participants were instructed to sink their hips into the harness to facilitate proper body line and fall procedure.
- Participants fell towards the mat covering the force plate. The participant's elbows were to remain fully extended during impact.

a) b)

Figure C1. a) Participant elevated prior to drop and b) immediately after landing. Padding was inserted under the participant's knees so as to maximize comfort during the drop testing. Two separate mats were placed under the participant's hands so as to maximize comfort during the landing phase of the drop testing, and to allow for differentiation between the floor and force plate, thereby minimizing double handed landings on the force plate.

APPENDIX D: VICON MOTION ANALYSIS MARKER PLACEMENT PROTOCOL

Vicon Marker Placement

The following is a description of the placement of the passive reflective infrared markers on the skin of the participants. Participants had 23 markers (14 mm in diameter) secured to their skin or clothing by means of clear, hypoallergenic two-sided tape along the right and left sides of the body. Markers in clusters were first secured to a rigid plastic body then to the participants, both using clear, hypoallergenic two-sided tape. The marker clusters were further secured to the arm by means of an elasticized cloth band and Velcro. The marker placement was as follows:

- *Right side:*
    - 1 marker on the hand along the third metacarpal,
    - 2 markers were attached to the wrist (radial and ulnar styloid processes),
    - Marker cluster (4 markers) on the forearm just inferior to the largest flexed portion of the extensor muscle belly on the posterior side of the forearm (in anatomical position),
    - 2 markers on the elbow (medial and lateral humeral epicondyles),
    - Marker cluster (4 markers) was attached to the upper arm segment just inferior to the largest flexed portion of the triceps brachii and just superior to the olecranon process, and
    - 1 marker was attached on the acromion process of the right shoulder.
    - 1 marker was attached to the right lateral femoral condyle.
- *Left side:*
    - 1 marker was attached to the wrist (ulnar styloid process),
    - 1 marker was attached to the elbow (lateral humeral epicondyle), and
    - 1 marker was attached on the acromion process of left shoulder.
    - 1 marker attached to the left lateral femoral condyle.
- Eight markers were used for the shoulder calibration only:
    - 2 markers attached to the wrist (radial and ulnar styloid processes),
    - 2 markers attached to the elbow (medial and lateral humeral epicondyles),
    - Chest cluster (4 markers) attached to the participants' shirt, just inferior to the sternal notch.

Figure D1. Lateral (left) and anterior (right) view of a harnessed participant with passive reflective infrared markers secured to skin. Calibration markers are still attached.

APPENDIX E: COMPARISON OF EXPERIMENTAL FORCES VERSUS FALL HEIGHT AND FORCES VERSUS IMPACT VELOCITY

Comparison of Experimental Forces Versus Fall Height and Impact Velocity

Conventionally, the forces (F_{1max} and F_{2max}) are presented relative to time. This comparison will yield the characteristic force profile plots, as in Figures 3b, 6, and 7. Comparison of peak forces to fall height, however, is required to determine the relation of the forces as fall height increases. It is difficult to precisely and accurately attain repeated falling heights. Further, these nominal fall heights are not specific to the individual; therefore, comparisons of the peak forces relative to impact velocity at the wrist and hand should be considered. However, for the general population, the use of impact velocity over fall height may not be clearly understood.

The impact velocity can be defined as the relative velocity of one mass (i.e., outstretched hand) to another (i.e., the ground) in an arbitrarily small time before the masses interact (i.e., the outstretched hand makes contact with the ground) (Serway & Jewett Jr., 2004). Impact velocity and fall height are exponentially related; that is, the impact velocity is the square of the fall height (Equations 12 and 13). Although impact velocity is difficult to repeat across time, it is specific to the individual (Table E1; Figures E1 and E2).

Table E1. Comparison of nominal fall height (cm), average (±SD) measured fall height (cm), and average (±SD) impact velocity (m/s). Not all trials were able to be analyzed because of high amounts of variability within the trials decreasing confidence in determining force peaks, the participants with one trial are labeled using *. The males are not highlighted and the females are

		Impact Velocity (m/s)				
Nominal Height (cm)	**Mean Actual Heights (cm)**	**Participant 1**	**Participant 2**	**Participant 3**	**Participant 4**	**Participant 5**
1	1.3 ± 0.5	0.50 ± 0.07	0.37 ± 0.18	0.21 ± 0.17	0.36 ± 0.08	0.93 ± 0.03
3	2.9 ± 0.4	0.72 ± 0.11	0.63 ± 0.05	0.63 ± 0.23	0.66 ± 0.02	0.96 ± 0.16
5	5.0 ± 0.4	1.10 ± 0.06	0.79 ± 0.12	0.98 ± 0.12	0.96 ± 0.08	1.53 ± 0.17
7	6.9 ± 0.4	1.33 ± 0.19	1.05 ± 0.17	1.33 ± 0.04	1.22 ± 0.03	1.63 ± 0.07
10	9.9 ± 0.6	1.61 ± 0.02	1.51 ± 0.15	1.50 ± 0.14	1.54 ± 0.07	1.90 ± 0.16
15	14.8 ± 0.8	1.51*	1.84 ± 0.09	1.87 ± 0.09	2.03 ± 0.09	2.40 ± 0.11
20	19.6 ± 0.6	1.54 ± 0.14	1.78 ± 0.09	2.19 ± 0.11	2.18 ± 0.08	2.50 ± 0.14
25	23.7 ± 1.7	1.94 ± 0.01	1.98 ± 0.10	2.37 ± 0.12	2.35 ± 0.09	2.61 ± 0.11

* Only one trial was considered good for analysis.

	Impact Velocity (m/s)				
Nominal Height (cm)	**Participant 6**	**Participant 7**	**Participant 8**	**Participant 9**	**Participant 10**
1	0.51 ± 0.23	0.25 ± 0.12	0.29 ± 0.11	0.32 ± 0.13	0.48 ± 0.3
3	0.63 ± 0.14	0.45 ± 0.14	0.51 ± 0.12	0.66 ± 0.13	0.72 ± 0.04
5	0.92 ± 0.17	0.87 ± 0.11	1.13 ± 0.23	1.06 ± 0.10	0.94 ± 0.03
7	1.35 ± 0.09	1.21 ± 0.03	1.42 ± 0.21	1.29 ± 0.11	1.19 ± 0.01
10	1.61 ± 0.11	1.59 ± 0.07	1.71 ± 0.21	1.62 ± 0.09	1.47 ± 0.12
15	1.89 ± 0.05	1.88 ± 0.18	1.86 ± 0.09	1.89 ± 0.08	1.92 ± 0.14
20	2.10 ± 0.06	2.08 ± 0.10	2.01 ± 0.03	1.88 ± 0.14	2.24 ± 0.11
25	2.20*	2.35*	2.16 ± 0.15	1.77 ± 0.08	2.32 ± 0.11

* Only one trial was considered good for analysis.

a)

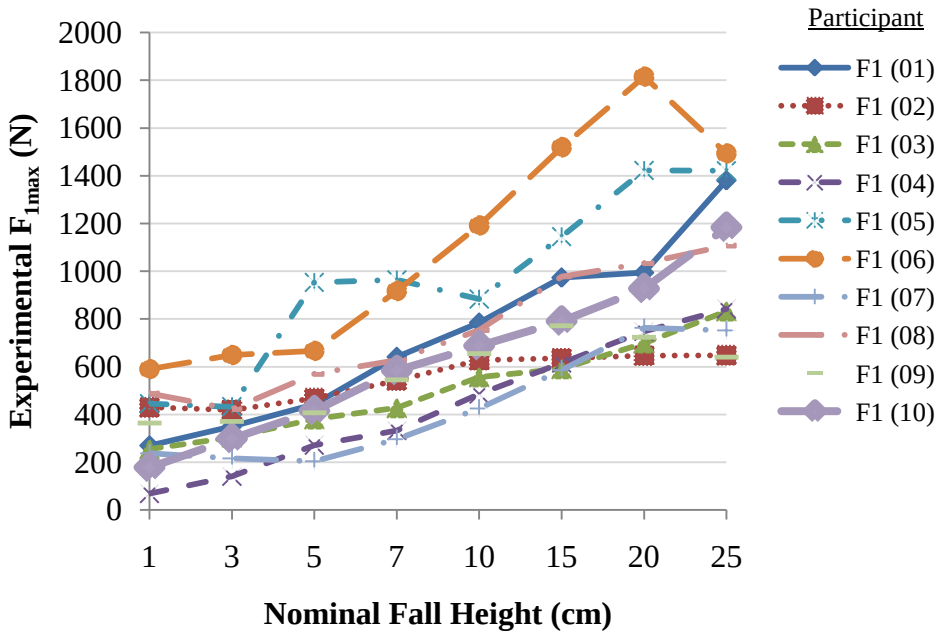

b)

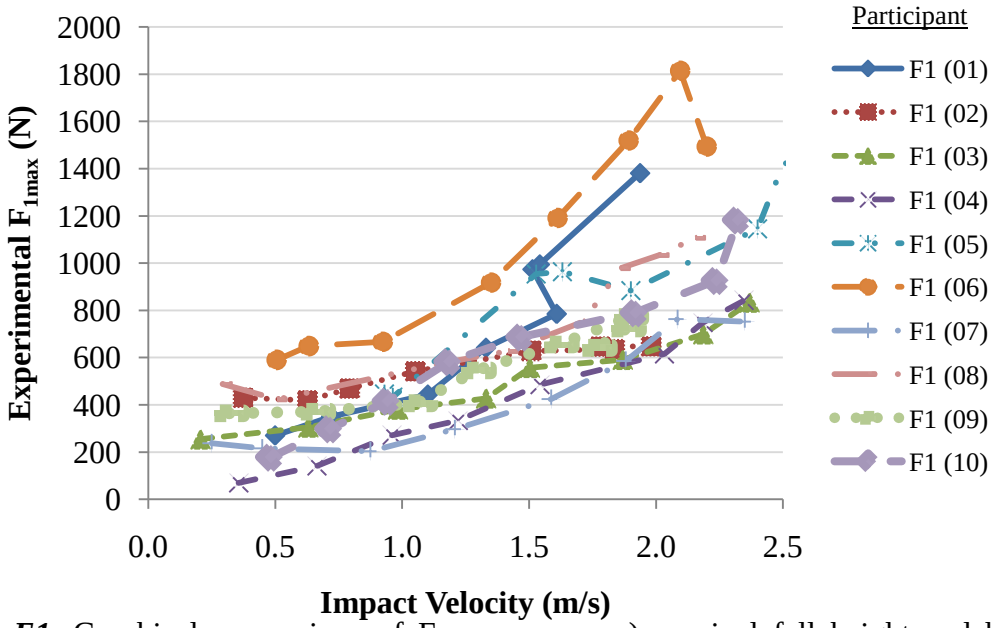

Figure E1. Graphical comparison of $F_{1max\text{-}E}$ versus a) nominal fall height and b) impact velocity.

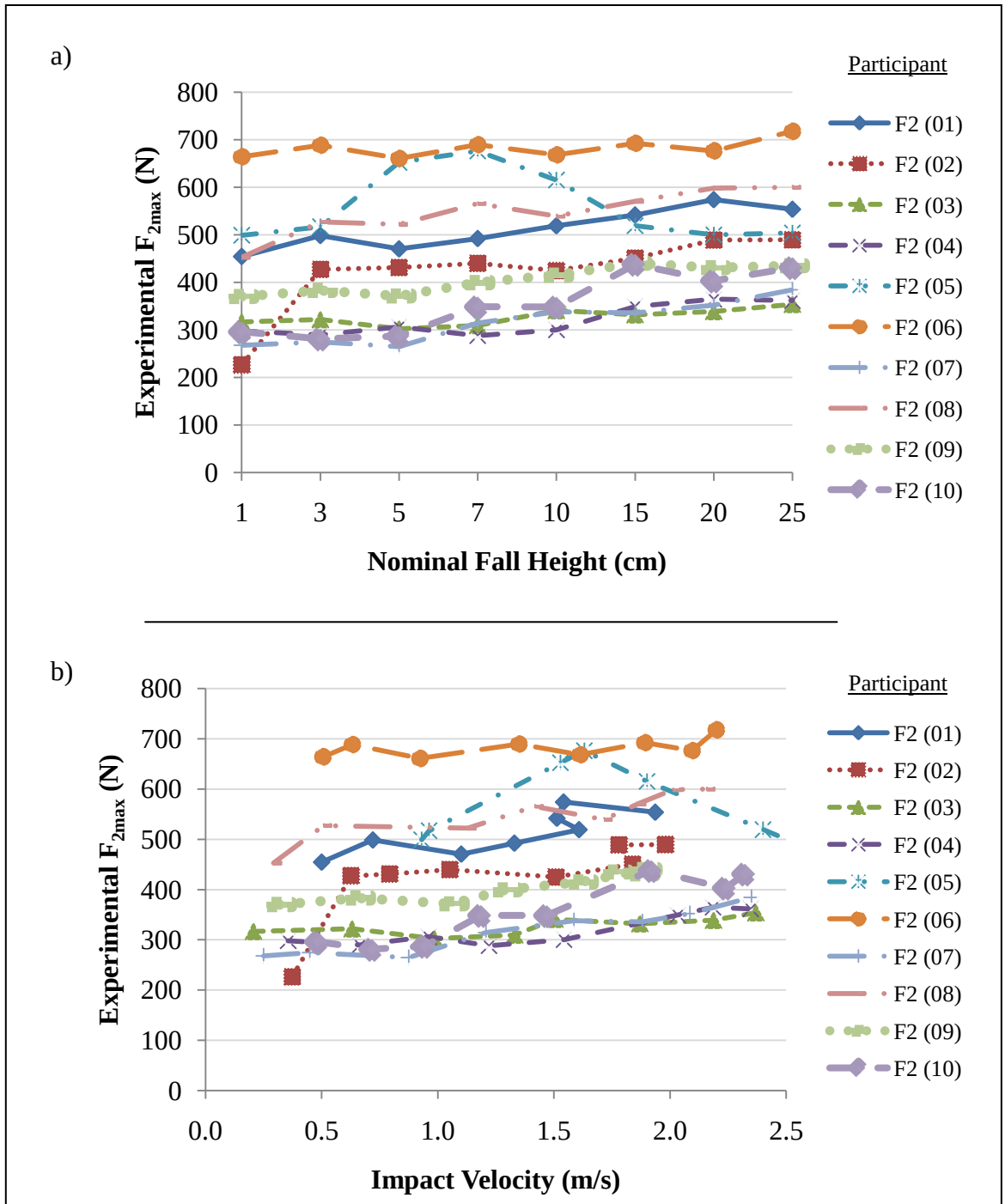

Figure E2. Graphical comparison of $F_{2max\text{-}E}$ versus a) nominal fall height and b) impact velocity.

APPENDIX F: PQCT MEASUREMENT PROTOCOL

pQCT Measurement Protocol

The following is a description of the body position and scanning procedure that the participant's were required to comply with during their participation in the study:

- Participants were seated in a chair with their dominant arm extended laterally through the gantry of the pQCT scanner. Their arm was positioned far enough into the gantry that their elbow was within the clamp.
- Arms were in the pronated position through the gantry and the hand was comfortably rested on the hand attachment.
- A foam cushion was placed on the arm rest, just under the participant's axilla, to ensure comfort.
- Participants were instructed to find a comfortable position and to sit as still as possible during the scanning period.
- Talking during the scanning period was not permitted so as to minimize movement artefact.
- A single scout scan was obtained prior to the scanning procedure in order to identify and reference the medial tip of the distal radius endplate.
- Scans were taken at 4% and 65% sites from the distal radius, as determined by the scout scan. At each site, a 2.3mm slice was obtained at a scanning speed of 20mm/s.

Figure F1. A participant seated for pQCT scanning of the dominant forearm (radius and ulna). The arm is extended laterally and pronated through the gantry. Foam support was placed under the participant armpit to maximize comfort.

Appendix G: PARTICIPANT SPECIFIC BONE AND MUSCLE DESCRIPTIVES

Participant Specific Descriptive Data

The following is a comprehensive report of all the bone and muscle descriptive data organized according to each participant involved in this study. These data were acquired using peripheral quantitative computed tomography (pQCT), a commonly used 3-dimensional bone and muscle x-ray imaging device. There are no standard deviations to report for this data because there was only one measurement session.

Table G1. Participant specific bone and muscle strength parameters, measured using peripheral quantitative computed tomography (pQCT). The males are not highlighted and the females are highlighted in grey.

	Participant									
Variables	**1**	**2**	**3**	**4**	**5**	**6**	**7**	**8**	**9**	**10**
Bone - 4% Site										
Total Area (ToA, mm^2)	538.24	321.60	356.96	329.44	410.88	538.88	300.80	571.04	353.44	444.16
Total Density (ToD, mg/cm^3)	383.20	391.70	334.70	376.40	349.50	406.00	361.50	373.00	313.60	300.80
Bone Strength Index (BSI_c, mg^2/cm^4)	79.04	49.34	39.99	46.67	50.19	88.83	39.31	79.45	34.76	40.19
Bone - 65% Site										
Cortical Area (CoA, mm^2)	156.80	117.28	105.92	109.60	133.60	169.28	104.64	182.72	114.24	131.04
Cortical Density (CoD, mg/cm^3)	905.80	995.40	870.90	968.10	836.50	863.20	915.60	786.70	853.70	958.00
Strength Strain Index (SSI_p, mm^3)	456.36	297.97	240.92	284.61	366.23	511.74	210.66	533.54	275.93	328.68
Muscle - 65% Site										
Total Area (ToA, mm^2)	5799.52	3255.36	3734.56	3084.96	5304.96	7534.24	3676.64	6640.96	3416.00	5364.48
Muscle Cross Sectional Area (MCSA, mm^2)	5628.00	3126.08	3615.20	2960.32	5148.00	7338.24	3560.96	6435.68	3289.60	5222.40

APPENDIX H: PARTICIPANT SPECIFIC ELBOW ANGLES

Participant Specific Elbow Angle Difference Between Trial Start and Impact

The elbow angle at impact was collected using the Vicon Nexus motion capture system. The elbow angle difference was calculated using Matlab. The program required marker information from the forearm marker cluster and the upper arm marker cluster. The average elbow angle differences between the trigger and ground impact are presented in below. The negative values indicate elbow flexion, while the positive values indicate elbow extension. The dotted line indicates the fall height at which the action at the elbow changes from flexion to extension. I reported sex separated and combined mean data for elbow angle differences because it is easier to see a trend (Table H1). However, I also reported participant specific elbow angle differences in Table H2. For all fall heights, the males had less elbow flexion relative to the females.

Table H1. Average (± SD) angle (degrees, ^{o}) difference between trigger and impact at the elbow for males, females, sexes pooled, and corresponding action at the elbow.

Nominal Height (cm)	**Average Elbow Angle Difference (^{o})**		**Average Elbow Angle Difference Combined (^{o}) (n = 10)**	**Action at Elbow**
	Males (n = 5)	**Females (n = 5)**		
1	-3.31 ± 0.53	-2.79 ± 1.49	-3.05 ± 1.09	Flexion
3	-2.21 ± 5.50	-5.40 ± 1.33	-5.00 ± 1.52	
5	-2.31 ± 6.15	-6.16 ± 2.85	-4.22 ± 4.96	
7	-2.07 ± 6.75	-4.36 ± 4.23	-3.14 ± 5.42	
10	-0.06 ± 5.31	-1.90 ± 4.43	-1.21 ± 4.89	
15	2.21 ± 6.06	0.23 ± 4.93	1.21 ± 5.32	Extension
20	3.68 ± 8.07	1.30 ± 4.06	3.18 ± 5.50	
25	3.78 ± 6.55	0.91 ± 4.98	3.06 ± 5.22	

Table H2. Comparison of nominal fall height (cm), and average (±SD) elbow angle difference among all participants in the study. The males are not highlighted and the females are highlighted in grey. The negative values indicate elbow flexion, while the positive values indicate elbow extension. If not asterisk (*) is by the number, then all trials were analyzed.

Nominal Height (cm)	**Average Elbow Angle Difference (°) for Participants:**									
	1	**2**	**3**	**4**	**5**	**6**	**7**	**8**	**9**	**10**
1	-3.94***	-4.76	-1.95	-3.49	-3.18***	-3.46***	-2.90	-2.50***	-0.83	-3.46
3	-4.34***	-7.05	-4.02	-6.42***	-2.11	-7.00	-5.28	-4.72***	-4.23	-4.80
5	-5.75***	-7.07	-3.00	-9.82	8.56	-5.22	-7.35	-5.68	-3.55	-3.28
7	-7.30**	-5.15	-0.01	-10.06	9.61	-2.54	-6.23	-5.34	-0.37	-4.02
10	-1.61**	-5.09	0.40	-7.02	9.11	-0.50	-1.96	-4.03	4.17	-5.60
15	2.28*	-1.59	1.04	-5.01	12.05	1.87	-1.45	-1.13	8.17	-4.10
20	4.09**	-1.44	0.74	-2.51	16.50	2.78	1.81	0.62	7.89	1.28
25	5.12**	-3.76	5.36	-2.78	13.85	2.09*	-1.41*	1.95	7.13**	3.02

* Involves only one analyzed trial

** Involves two analyzed trials

*** Involves three analyzed trials

APPENDIX I: TIME TO IMPACT

Time to Impact

Time to impact was collected using both the Vicon Nexus motion capture system and the integrated force plate information. In order to obtain the time to impact, I marked the positive inflection point of the force profile that was inputted into Matlab from the force plate. The positive inflection point corresponded to the instant that there was pressure on the force plate (i.e., the moment of contact). Matlab was used to calculate the corresponding time between the start of the trial and the positive inflection point (i.e., ground impact). The average impact time across all fall heights is presented in Table I1. In general, the time to impact increased with increasing fall height for both males and females.

Table I1. Average (± SD) time to impact from the start of the trial for all fall heights.

Nominal Height (cm)	**Average Impact Time (ms)**		**Average Impact Time (ms) (n = 10)**
	Males (n = 5)	**Females (n = 5)**	
1	1089.01 ± 11.94	1076.24 ± 16.28	1082.63 ± 14.11
3	1095.37 ± 21.53	1103.39 ± 13.36	1099.38 ± 17.45
5	1117.89 ± 15.29	1125.61 ± 10.82	1121.75 ± 13.06
7	1136.60 ± 10.73	1136.52 ± 9.37	1136.56 ± 9.97
10	1152.63 ± 12.08	1150.80 ± 10.15	1151.72 ± 11.12
15	1175.22 ± 6.48	1175.35 ± 9.48	1175.29 ± 8.15
20	1192.66 ± 7.57	1202.72 ± 9.33	1197.69 ± 8.45
25	1205.30 ± 9.04	1224.29 ± 9.51	1214.79 ± 9.27

APPENDIX J: PARTICIPANT SPECIFIC FORCES: EXPERIMENTAL AND MODEL

Participant Specific Forces: Experimental and Model

Forces were collected experimentally using the force plate, and mathematically predicted using the two-mass, spring-damper model. I averaged the experimental and model force data from each of the fall trials for ever fall height and for every participant. I report the $F_{1max\text{-}E}$ and $F_{1max\text{-}M}$ in Tables J2 and J3, respectively. I report $F_{2max\text{-}E}$ and $F_{2max\text{-}M}$ in Tables J4 and J5 respectively. For comparative purposes, I report the experimental and model forces, not controlling for mass; these force data are reported separated sex (Table J1).

Table J1. Average (± SD) force outputs from experimentation and the mathematical model for all participants at the different fall heights. Forces are not controlled for body mass.

	Experimental Forces		***Model Forces***	
	Males (n=5)	**Females (n = 5)**	**Males (n=5)**	**Females (n = 5)**
F1 (N)				
1 cm	394.48 ± 167.27	271.02 ± 137.92	290.82 ± 121.09	155.12 ± 29.23
3 cm	430.52 ± 133.72	290.44 ± 113.01	375.82 ± 83.65	298.48 ± 41.91
5 cm	609.86 ± 217.18	346.37 ± 106.92	600.32 ± 133.52	463.17 ± 51.37
7 cm	746.75 ± 179.14	429.21 ± 115.06	744.44 ± 95.81	613.05 ± 56.89
10 cm	860.24 ± 198.20	550.05 ± 96.19	898.57 ± 96.37	789.25 ± 32.62
15 cm	1081.44 ± 275.11	640.10 ± 76.38	1044.51 ± 186.73	977.93 ± 13.97
20 cm	1231.61 ± 375.66	716.11 ± 45.96	1137.25 ± 208.19	1043.58 ± 90.38
25 cm	1317.34 ± 164.28	743.46 ± 76.73	1232.39 ± 146.38	1121.70 ± 143.93
F2 (N)				
1 cm	473.34 ± 131.57	295.81 ± 53.82	637.75 ± 91.51	455.42 ± 56.23
3 cm	502.60 ± 145.29	339.37 ± 64.50	650.98 ± 86.53	474.91 ± 55.47
5 cm	518.65 ± 153.29	335.27 ± 65.93	708.63 ± 93.66	513.23 ± 52.79
7 cm	554.49 ± 140.88	350.33 ± 65.64	753.74 ± 102.01	559.92 ± 54.82
10 cm	538.16 ± 121.71	363.80 ± 53.85	810.60 ± 103.00	624.40 ± 53.18
15 cm	552.42 ± 92.48	381.65 ± 58.73	869.96 ± 128.77	700.98 ± 37.84
20 cm	550.41 ± 103.78	395.15 ± 63.36	908.84 ± 138.13	728.95 ± 49.33
25 cm	561.34 ± 107.56	404.95 ± 56.99	948.45 ± 115.42	762.70 ± 70.15

Table J2. Average (± SD) experimental, mass controlled force outputs for all participants at the different fall heights. The males are not highlighted and the females are highlighted in grey.

Nominal Height (cm)	Mass controlled experimental F_{1max} (N/kg) data						
	1	**2**	**3**	**4**	**5**	**6**	**7**
1	3.72 ± 0.06***	6.14 ± 0.44	3.74 ± 0.31	1.36 ± 0.21	5.40 ± 0.97***	5.84 ± 0.57***	3.67 ± 0.16
3	4.83 ± 0.48***	5.99 ± 0.68	4.48 ± 1.11	2.77 ± 0.41***	5.24 ± 1.90	6.42 ± 0.52	3.34 ± 0.40
5	6.11 ± 0.97***	6.70 ± 0.19	5.60 ± 0.46	5.33 ± 0.74	11.56 ± 1.30	6.60 ± 0.51	3.16 ± 0.67
7	8.85 ± 2.20**	7.75 ± 0.40	6.29 ± 0.30	6.53 ± 0.44	11.68 ± 1.58	9.09 ± 1.18	4.61 ± 0.81
10	10.83 ± 3.03**	8.97 ± 0.56	8.19 ± 1.83	9.52 ± 1.67	10.71 ± 0.34	11.80 ± 1.00	6.59 ± 0.74
15	13.43*	9.09 ± 0.67	8.69 ± 0.86	12.07 ± 0.76	13.88 ± 1.03	15.04 ± 0.77	9.09 ± 0.88
20	13.72 ± 0.11	9.24 ± 0.35	10.28 ± 0.65	14.67 ± 0.79	17.24 ± 2.77	17.97 ± 0.52	11.83 ± 1.04
25	19.05 ± 0.60	9.26 ± 1.27	12.25 ± 1.93	16.52 ± 0.63	17.23 ± 1.88*	14.79*	11.67*

* Involves only one analyzed trial
** Involves two analyzed trials
*** Involves three analyzed trials

Nominal Height (cm)	Mass controlled experimental F_{1max} (N/kg) data		
	8	**9**	**10**
1	5.40 ± 0.92***	5.69 ± 0.24	2.35 ± 0.85
3	4.67 ± 0.19***	5.80 ± 0.38	3.93 ± 0.18
5	6.30 ± 0.86	6.36 ± 0.30	5.47 ± 0.70
7	6.93 ± 0.58	8.52 ± 0.78	7.68 ± 0.75
10	8.33 ± 0.73	10.23 ± 0.58	9.05 ± 1.73
15	10.81 ± 1.33	12.06 ± 0.53	10.40 ± 1.41
20	11.43 ± 1.73	11.31 ± 1.50	12.20 ± 0.30
25	12.24 ± 3.50	10.02 ± 1.01**	15.57 ± 1.38

* Involves only one analyzed trial
** Involves two analyzed trials
*** Involves three analyzed trials

Table J3. Average (± SD) model predicted, mass controlled force outputs for all participants at the different fall heights. The males are not highlighted and the females are highlighted in grey.

Nominal Height (cm)	Mass controlled model predicted F_{1max} (N/kg) data									
	1	**2**	**3**	**4**	**5**	**6**	**7**	**8**	**9**	**10**
1	3.54	2.74	1.74	3.32	5.97	2.84	2.06	1.86	2.55	3.29
3	5.08	4.56	4.65	6.02	6.17	3.47	3.48	3.07	5.09	4.91
5	7.83	5.73	7.30	8.88	9.97	5.05	6.73	6.78	8.30	6.43
7	9.55	7.68	10.03	11.43	10.65	7.45	9.47	8.58	10.18	8.19
10	11.65	11.21	11.38	14.62	12.49	8.93	12.61	10.39	12.94	10.21
15	10.90	13.79	14.36	19.64	15.95	10.54	15.06	11.34	15.23	13.50
20	11.12	13.32	16.95	21.22	16.65	11.75	16.76	12.29	15.15	15.88
25	14.18	14.89	18.43	23.01	17.43	12.33	19.06	13.25	14.21	16.47

Table J4. Average (± SD) experimental, weight controlled force outputs for all participants at the different fall heights. The males are not highlighted and the females are highlighted in grey.

Nominal Height (cm)	Mass controlled experimental F_{2max} (N/kg) data						
	1	**2**	**3**	**4**	**5**	**6**	**7**
1	6.27 ± 0.89***	3.23 ± 0.27	4.66 ± 0.59	5.84 ± 0.40	6.05 ± 0.38***	6.58 ± 0.12***	4.15 ± 0.33
3	6.88 ± 0.24***	6.10 ± 0.28	4.73 ± 0.40	5.68 ± 0.50***	6.27 ± 1.23	6.82 ± 0.20	4.26 ± 0.39
5	6.49 ± 0.25***	6.16 ± 0.53	4.45 ± 0.44	6.01 ± 0.59	7.91 ± 0.57	6.54 ± 0.16	4.10 ± 0.54
7	6.79 ± 0.58**	6.28 ± 0.39	4.55 ± 0.33	5.65 ± 0.20	8.20 ± 1.25	6.83 ± 0.17	4.88 ± 0.39
10	7.16 ± 0.51**	6.07 ± 0.11	5.01 ± 0.66	5.88 ± 0.65	7.46 ± 1.16	6.62 ± 0.38	5.24 ± 0.66
15	7.47*	6.44 ± 0.23	4.88 ± 0.62	6.85 ± 0.62	6.29 ± 0.57	6.86 ± 0.62	5.21 ± 0.81
20	7.92 ± 0.21**	6.99 ± 0.21	4.98 ± 0.91	7.15 ± 0.49	6.06 ± 0.35	6.70 ± 0.63	5.46 ± 0.42
25	7.64 ± 0.49**	6.99 ± 0.21	5.20 ± 0.72	7.09 ± 0.48	6.11 ± 0.11	7.11*	5.96*

* Involves only one analyzed trial
** Involves two analyzed trials
*** Involves three analyzed trials

Nominal Height (cm)	Mass controlled experimental F_{2max} (N/kg) data		
	8	**9**	**10**
1	5.00 ± 0.59***	5.78 ± 0.24	3.90 ± 0.27
3	5.83 ± 0.24***	5.99 ± 0.26	3.70 ± 0.46
5	5.77 ± 0.58	5.81 ± 0.35	3.78 ± 0.59
7	6.25 ± 0.38	6.24 ± 0.20	4.59 ± 0.36
10	5.96 ± 0.31	6.49 ± 0.38	4.58 ± 0.41
15	6.30 ± 0.70	6.88 ± 0.40	5.76 ± 1.16
20	6.61 ± 0.45	6.74 ± 0.63	5.30 ± 0.90
25	6.63 ± 0.15	6.80 ± 0.23**	5.67 ± 0.75

Table J5. Average (± SD) model predicted, mass controlled force outputs for all participants at the different fall heights. The males are not highlighted and the females are highlighted in grey.

	Mass controlled model predicted F_{2max} (N/kg) data									
Nominal Height (cm)	**1**	**2**	**3**	**4**	**5**	**6**	**7**	**8**	**9**	**10**
1	7.39	7.26	7.16	7.09	8.00	7.57	7.14	7.37	7.18	7.39
3	7.66	7.52	7.51	7.53	8.05	7.66	7.29	7.51	7.54	7.67
5	8.37	7.76	8.14	8.30	9.28	7.99	7.92	8.33	8.36	8.02
7	8.93	8.28	9.02	9.16	9.53	8.70	8.75	8.92	8.99	8.54
10	9.71	9.48	9.51	10.41	10.27	9.22	9.91	9.59	10.03	9.24
15	9.42	10.51	10.69	12.52	11.74	9.86	10.89	9.97	10.96	10.53
20	9.51	10.31	11.79	13.20	12.05	10.36	11.61	10.36	10.92	11.53
25	10.72	10.96	12.43	13.98	12.39	10.61	12.61	10.77	10.54	11.79

APPENDIX K: CERTIFICATE OF ETHICAL APPROVAL

UNIVERSITY OF SASKATCHEWAN

Biomedical Research Ethics Board (Bio-REB)

Certificate of Approval
Study Amendment

PRINCIPAL INVESTIGATOR	DEPARTMENT	Bio #
Joel Lanovaz	Kinesiology	09-108

INSTITUTION(S) WHERE RESEARCH WILL BE CARRIED OUT
Physical Activity Complex (PAC)
University of Saskatchewan
Saskatoon SK

SUB-INVESTIGATOR(S)
James Johnston, Saija Kontulainen

STUDENT RESEARCHER(S)
Devin Glennie, Chantal Kawalilak, David Kobylak

SPONSORING AGENCIES
UNFUNDED

TITLE
: Validation of Fall Impact Force Prediction Model

APPROVAL OF	APPROVED ON	CURRENT EXPIRY DATE
Researcher's Summary v.2 (11-Aug-2010) Research Participant Information and Consent Form v.3 (11-Aug-2010)	12-Aug-2010	26-May-2011

Delegated Review: ☒ Full Board Meeting: ☐

CERTIFICATION
The study is acceptable on scientific and ethical grounds. The Bio-REB considered the requirements of section 29 under the Health Information Protection Act (HIPA) and is satisfied that this study meets the privacy considerations outlined therein. The principal investigator has the responsibility for any other administrative or regulatory approvals that may pertain to this research study, and for ensuring that the authorized research is carried out according to governing law. This approval is valid for the specified period provided there is no change to the approved protocol or consent process.

FIRST TIME REVIEW AND CONTINUING APPROVAL
The University of Saskatchewan Biomedical Research Ethics Board reviews above minimal studies at a full-board (face-to-face) meeting. Any research classified as minimal risk is reviewed through the delegated (subcommittee) review process. The initial Certificate of Approval includes the approval period the REB has assigned to a study. The Status Report form must be submitted within one month prior to the assigned expiry date. The researcher shall indicate to the REB any specific requirements of the sponsoring organizations (e.g. requirement for full-board review and approval) for the continuing review process deemed necessary for that project. For more information visit http://www.usask.ca/research/ethics_review/.

REB ATTESTATION
In respect to clinical trials, the University of Saskatchewan Research Ethics Board complies with the membership requirements for Research Ethics Boards defined in Division 5 of the Food and Drug Regulations and carries out its functions in a manner consistent with Good Clinical Practices. This approval and the views of this REB have been documented in writing.

Gordon McKay, Ph.D., Vice-Chair
University of Saskatchewan
Biomedical Research Ethics Board

Please send all correspondence to:
Research Ethics Office
University of Saskatchewan
Box 5000 RPO University
1607-110 Gymnasium Place
Saskatoon SK S7N 4J8